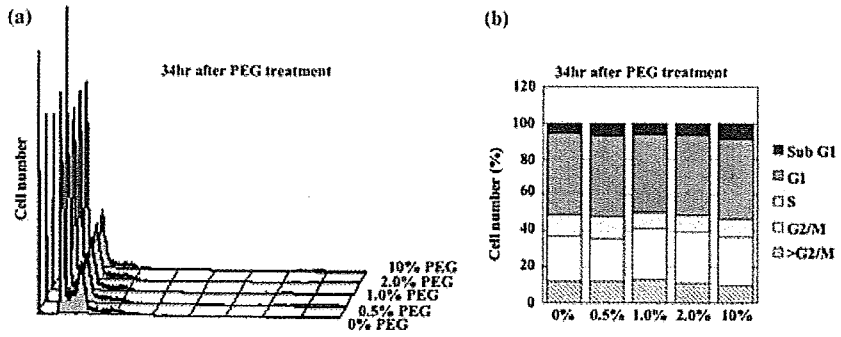

Fig. 6. Cell cycle analysis. (a) Cell cycle profiles after polyethylene glycol (PEG) treatment at 34 h are demonstrated. (b) From the data sets presented in (a), the cell population of each fraction (sub-G_1, G_1, S, G_2/M, and > G_2/M fraction) in the cell cycle is shown.

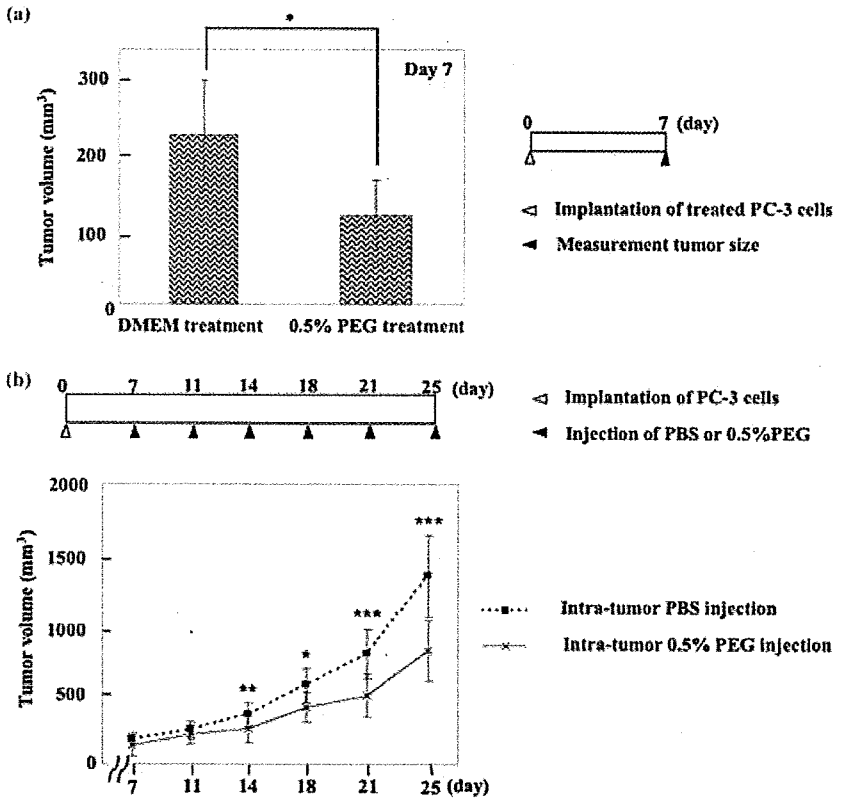

Fig. 7. Growth-suppressive effects of 0.5% polyethylene glycol (PEG) on PC-3 xenografts in nude mice. (a) After PC-3 cells were treated with Dulbecco's modified Eagle's medium (DMEM) or 0.5% PEG for 30 min, the cells were implanted into the backs of nude mice at day 0. Tumor volumes were measured at day 7. (b) Experimental protocols. PC-3 cells were implanted into backs of nude mice at day 0, and then 200 μL aliquots of phosphate-buffered saline (PBS) or 0.5% PEG was injected into palpable tumors twice a week during 19 days (top). Growth curves on PC-3 xenografts injected with PBS (■) or 0.5% PEG (X) are demonstrated (bottom). Values are the mean of fold ± SD. $*P < 0.05$, $**P < 0.01$, $***P < 0.001$.

day 25 (Fig. 7b bottom). No significant change in bodyweight was observed between the two groups during the experimental period (data not shown). Histopathological analysis revealed the presence of vacant spaces in tumors at the site of injection (Fig. 8a–d). Multinucleated cells were frequently observed surrounding these spaces in PEG-injected groups, and multinucleated cells were observed in approximately 20% of the total TUNEL-positive cells. In contrast, few TUNEL-positive cells were detected in PBS-injected tumors, although necrotic lesions were similarly observed. Multinucleated cells were rarely apparent in PBS-injected tumors (Fig. 8c,e).

Discussion

The present study demonstrated the antitumor effects of PEG via multinucleated cell formation, presumably though the induction of cell fusion. This is in line with the recent report by Roy *et al.* that PEG 800 induces apoptosis in two human colonic adenocarcinoma cells, HT29 and CaCo-2, at concentrations of 3.6–4.8%.[35] Although they briefly described PEG-induced cell fusion to be a possible mechanism, they considered this unlikely because a much higher concentration of PEG, around 30–50%, is generally required to induce cell fusion.[35]

In the present study, we were indeed able to demonstrate that low concentrations of PEG could induce apoptosis via multinucleated cell formation. More surprisingly, nuclear condensation was evident in a fraction of the multinucleated cells. As it has been reported that the cell-fusion process occurs within 1–2 h, mitotic catastrophe should be considered as a causative event for the induction of cell death by PEG.[36] However, the number of aneuploid cells in the > G_2/M fraction did not show a significant change during this time, and the number of large multinucleated cells decreased between 34 and 36 h. Therefore, an abrupt decrease in cell numbers after PEG treatment of PC-3 cells *in vitro* is reasonably explained by the induction of apoptosis in multinucleated cells, although clumped cells with aneuploid

doi: 10.1111/j.1349-7006.2008.00781.x

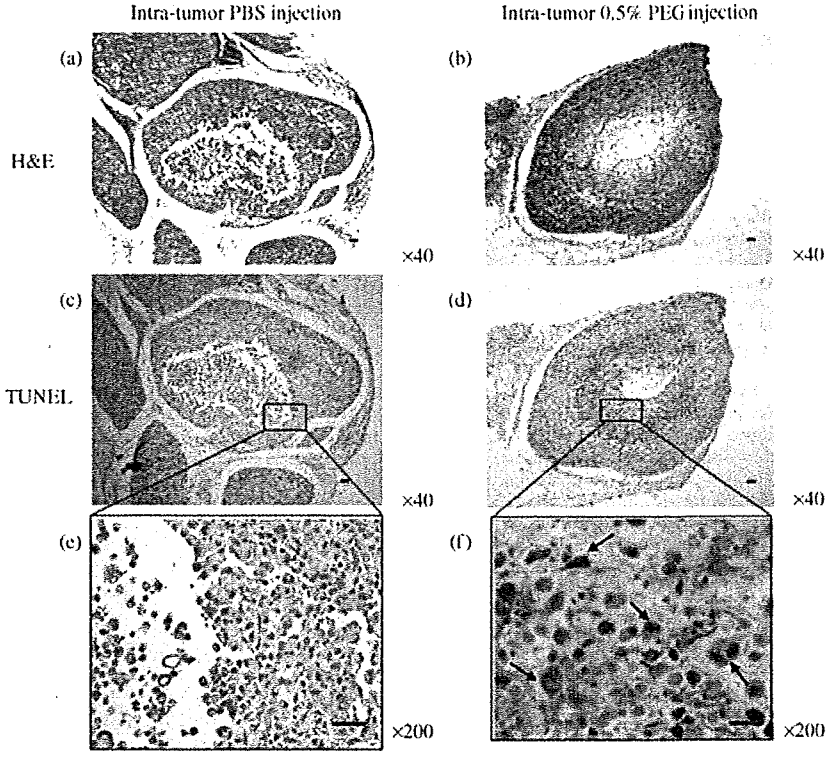

Fig. 8. Induction of multinucleated cells and apoptosis by polyethylene glycol (PEG) injection in PC-3 xenografts. Tumors with similar sizes were selected and allotted randomly into two groups. Aliquots (200 μL) of phosphate-buffered saline (PBS) or 0.5% PEG were injected directly into each group of tumors at days 7, 11, 14, 18, 21, and 25. Representative histological features of tumors in experimental groups of (a,c,e) PBS injection and (b,d,f) PEG injection are presented. The tumor sizes at day 7 before the PBS and 0.5% PEG injections were 180 ± 42 and 140 ± 70 mm^3, respectively. (a,b) Hematoxylin and eosin (H&E) staining. (c–f) TdT-mediated dUTP-biotin nick end-labeling (TUNEL) immunohistochemical staining. (e,f) Magnified images of (c) and (d), respectively. The arrows indicate typical multinucleated cells positive for TUNEL staining. Scale bars = 50 μm.

characteristics may also be a part of the large-cell fraction. Further work is needed to substantiate this possibility, but the positive staining for Annexin-V and PI and PARP-1 cleavage provide some support for this hypothesis.

Taking the results together, it is plausible that multinucleated cell formation is a trigger and causative event for the induction of apoptosis by PEG. Although an increase in osmotic pressure by PEG has been considered to be important for its cytostatic or apoptotic effects,[35] it is unlikely that osmotic pressure played a role with the low concentrations of PEG used here. Indeed, when PC-3 cells were cultured in the presence of PEG under ordinary culture conditions, we did not detect apparent changes in cell-growth properties for up to 72 h (Fig. 2a). This negates the possible implication of osmotic pressure in the induction of apoptosis by the concentrations of PEG used in the present conditions. Another possibility to be considered is that cell-membrane damage caused by PEG led to the induction of apoptosis. It is thought that the cell membrane could be damaged by injection of cells with PEG particles through microcylinders in *in vivo* models. Further study is warranted to corroborate or refute this point. However, the induction of nuclear condensation, positive staining for Annexin-V in multinucleated cells, and PARP-1 cleavage by PEG treatment all point to a significant role for apoptosis in the growth-suppressive effects of PEG. Although the mechanism of induction of apoptosis by PEG remains unclear, we clearly demonstrated that PEG exhibited a suppressive effect on tumor growth *in vivo* and induced apoptosis, possibly via the cell-fusion mechanism.

Lastly, we should note that PC-3 prostate cancer cells were used as a model system. The therapies for prostate cancer, for example hormone therapy or radiation therapy, have some drawbacks. Radioactive material such as iodine-125 using brachytherapy may cause chromosomal aberrations.[37] Occurrence of androgen-independent prostate cancers because of frequent or continuous application of hormone therapy is a very serious problem at present. Once cancer becomes androgen independent, metastatic lesions manifest aggressively within 12–18 months, and the average patient survival time is only 2–3 years.[38] Although chemotherapies have been adapted for androgen-independent aggressive cancer cases, the tumor-suppressive effects brought about by those therapies are not satisfactory.[39] Therefore, for cases with localized non-invasive lesions, urologists generally choose radical prostatectomy.[40] At the same time, however, there are a substantial number of cases in which radical therapy cannot be conducted because of the poor compliance of patients and life-threatening side effects.[41,42]

In the present study, we clearly demonstrated that PEG is able to induce apoptosis in PC-3 cells in an autonomous cell-fusion manner, with efficient suppression of tumor growth *in vivo*. Based on our observations, we propose that direct intratumoral injection of PEG could be a promising therapeutic approach for androgen-independent prostate cancers. Clearly, if PEG is injected in clinical trials, it may induce cell fusion for normal prostate cells, and unwanted side effects may appear. However, even if PEG induces multinucleated cells between normal and tumor cells, it could be effective for diffuse types of prostate cancer. In addition, direct intratumoral injection of PEG could also assist hormone therapy and radiation therapy. Although several problems remain to be solved, the potential of PEG as a novel, non-invasive and non-toxic therapeutic agent clearly warrants further attention.

Acknowledgments

The authors thank Masako Ochiai and Ibuki Kobayashi (Biochemistry Division, National Cancer Center Research Institute) for technical help and discussion throughout this study. This work was supported in part by a Grant-in-Aid for the Third-Term Comprehensive 10-Year Strategy for Cancer Control from the Ministry of Health, Labour, and Welfare of Japan, and in part by a Grant-in-Aid for Cancer Research from the Ministry of Health, Labour, and Welfare of Japan. K. F. was a recipient of a Research Resident Fellowship from the Foundation for Promotion of Cancer Research in Japan during the research.

References

1 Schiller LR, Emmett M, Santa Ana CA, Fordtran JS. Osmotic effects of polyethylene glycol. *Gastroenterology* 1988; **94**: 933–41.
2 Elsenhans B, Caspary WF. Differential changes in the urinary excretion of two orally administered polyethylene glycol markers (PEG 900 and PEG 4000) in rats after feeding various carbohydrate gelling agents. *J Nutr* 1989; **119**: 380–7.
3 Hunnuksela M, Pirila V, Salo OP. Skin reactions to propylene glycol. *Contact Dermatitis* 1975; **1**: 112–16.
4 Ramkumar D, Rao SS. Efficacy and safety of traditional medical therapies for chronic constipation: systematic review. *Am J Gastroenterol* 2005; **100**: 936–71.
5 Quartier S, Garmyn M, Becart S, Goossens A. Allergic contact dermatitis to copolymers in cosmetics – case report and review of the literature. *Contact Dermatitis* 2006; **55**: 257–67.
6 Veronese FM, Pasut G. PEGylation, successful approach to drug delivery. *Drug Discov Today* 2005; **10**: 1451–8.
7 Molineux G. Pegylation: engineering improved pharmaceuticals for enhanced therapy. *Cancer Treat Rev* 2002; **28**: 13–16.
8 Rassoulzadegan M, Binetruy B, Cuzin F. High frequency of gene transfer after fusion between bacteria and eukaryotic cells. *Nature* 1982; **295**: 257–9.
9 Chiu DT. A microfluidics platform for cell fusion. *Curr Opin Chem Biol* 2001; **5**: 609–12.
10 Naigamwalla D, Chia MC, Tran TT *et al.* Polyethylene glycol 8000 and colon carcinogenesis: inhibition in the F344 rat, promotion in the Min mouse. *Cancer Res* 2000; **60**: 6856–8.
11 Corpet DE, Parnaud G, Delverdier M, Peiffer G, Tache S. Consistent and fast inhibition of colon carcinogenesis by polyethylene glycol in mice and rats given various carcinogens. *Cancer Res* 2000; **60**: 3160–4.
12 Nakagama H, Nakanishi M, Ochiai M. Modeling human colon cancer in rodents using a food-borne carcinogen, PhIP. *Cancer Sci* 2005; **96**: 627–36.
13 Klurfeld DM. Dietary fiber-mediated mechanisms in carcinogenesis. *Cancer Res* 1992; **52**: 2055S–9S.
14 Parnaud G, Tache S, Peiffer G, Corpet DE. Polyethylene-glycol suppresses colon cancer and causes dose-dependent regression of azoxymethane-induced aberrant crypt foci in rats. *Cancer Res* 1999; **59**: 5143–7.
15 Roy HK, Gulizia J, DiBaise JK *et al.* Polyethylene glycol inhibits intestinal neoplasia and induces epithelial apoptosis in Apc (min) mice. *Cancer Lett* 2004; **215**: 35–42.
16 Webber MM, Bello D, Quader S. Immortalized and tumorigenic adult human prostatic epithelial cell lines. characteristics and applications. Part I. Cell markers and immortalized nontumorigenic cell lines. *Prostate* 1996; **29**: 386–94.
17 Ahmedin J, Rebecca S, Elizabeth W, Taylor M, Jiaquan X, Michael JT. Cancer statistics, 2007. *CA Cancer J Clin* 2007; **57**: 43–66.
18 Marugame T, Mizuno S. Comparison of prostate cancer mortality in five countries. France, Italy, Japan, UK and USA from the WHO mortality database (1960–2000). *Jpn J Clin Oncol* 2005; **35**: 690–1.
19 Huggins C, Hodges CV. Studies on prostate cancer: effect of castration, estrogen and androgen injection on serum phosphatases in metastatic carcinoma of the prostate. *Cancer Res* 1941; **1**: 293–7.
20 Singh P, Uzgare A, Litvinov I, Denmeade SR, Isaacs JT. Combinatorial androgen receptor targeted therapy for prostate cancer. *Endocr Relat Cancer* 2006; **13**: 653–66.
21 Di Lorenzo G, Autorino R, Figg WD, De Placido S. Hormone-refractory prostate cancer: where are we going? *Drugs* 2007; **67**: 1109–24.
22 Randy VH. Modern brachytherapy for treatment of prostate cancer. *Cancer Control* 2007; **14**: 238–43.
23 Scher HI, Kelly WK. Flutamide withdrawal syndrome: its impact on clinical trials in hormone-refractory prostate cancer. *J Clin Oncol* 1993; **11**: 1566–72.
24 Laboisse CL, Maoret JJ, Triadou N, Augeron C. Restoration by polyethylene glycol of characteristics of intestinal differentiation in subpopulations of the human colonic adenocarcinoma cell line HT29. *Cancer Res* 1988; **48**: 2498–504.
25 Bindu L, Balaram P, Mathew A, Remani P, Bhattathiri VN, Nair MK. Radiation-induced changes in oral carcinoma cells – a multiparametric evaluation. *Cytopathology* 2003; **14**: 287–93.
26 Liu MJ, Wang Z, Ju Y, Zhou JB, Wang Y, Wong RN. The mitotic-arresting and apoptosis-inducing effects of diosgenyl saponins on human leukemia cell lines. *Biol Pharm Bull* 2004; **27**: 1059–65.
27 Makarovskiy AN, Siryaporn E, Hixson DC, Akerley W. Survival of docetaxel-resistant prostate cancer cells *in vitro* depends on phenotype alterations and continuity of drug exposure. *Cell Mol Life Sci* 2002; **59**: 1198–211.
28 Tsuchiya N, Fukuda H, Sugimura T, Nagao M, Nakagama H. LRP130, a protein containing nine pentatricopeptide repeat motifs, interacts with a single-stranded cytosine-rich sequence of mouse hypervariable minisatellite Pc-1. *Eur J Biochem* 2002; **269**: 2927–33.
29 Shimada K, Nakamura M, Ishida E, Kishi M, Yonehara S, Konishi N. c-Jun NH2-terminal kinase-dependent Fas activation contributes to etoposide-induced apoptosis in p53-mutated prostate cancer cells. *Prostate* 2003; **55**: 265–80.
30 Obasaju C, Hudes GR. Paclitaxel and docetaxel in prostate cancer. *Hematol Oncol Clin North Am* 2001; **15**: 525–45.
31 van Engeland M, Nieland LJ, Ramaekers FC, Schutte B, Reutelingsperger CP. Annexin V-affinity assay: a review on an apoptosis detection system based on phosphatidylserine exposure. *Cytometry* 1998; **31**: 1–9.
32 Gavrieli Y, Sherman Y, Ben-Sasson SA. Identification of programmed cell death *in situ* via specific labeling of nuclear DNA fragmentation. *J Cell Biol* 1992; **119**: 493–501.
33 Bedner E, Li X, Gorczyca W, Melamed MR, Darzynkiewicz Z. Analysis of apoptosis by laser scanning cytometry. *Cytometry* 1999; **35**: 181–95.
34 Soldani C, Scovassi AI. Poly (ADP-ribose) polymerase-1 cleavage during apoptosis: an update. *Apoptosis* 2002; **7**: 321–8.
35 Roy HK, DiBaise JK, Black J, Karolski WJ, Ratashak A, Ansari S. Polyethylene glycol induces apoptosis in HT-29 cells: potential mechanism for chemoprevention of colon cancer. *FEBS Lett* 2001; **496**: 143–6.
36 Lentz BR. PEG as a tool to gain insight into membrane fusion. *Eur Biophys J* 2007; **36**: 315–26.
37 Arslan NC, Geard CR, Hall EJ. Low dose-rate effects of cesium-137 and iodine-125 on cell survival, cell progression, and chromosomal alterations. *Am J Clin Oncol* 1986; **9**: 521–6.
38 Chang SS. Treatment options for hormone-refractory prostate cancer. *Rev Urol* 2007; **9**: S13–18.
39 Oh WK, Tay MH, Huang J. Is there a role for platinum chemotherapy in the treatment of patients with hormone-refractory prostate cancer? *Cancer* 2007; **109**: 477–86.
40 Freedland SJ, Moul JW. Prostate specific antigen recurrence after definitive therapy. *J Urol* 2007; **177**: 1985–91.
41 Augustin H, Hammerer P, Graefen M *et al.* Intraoperative and perioperative morbidity of contemporary radical retropubic prostatectomy in a consecutive series of 1243 patients: results of a single center between 1999 and 2002. *Eur Urol* 2003; **43**: 113–18.
42 Benoit RM, Naslund MJ, Cohen JK. Complications after radical retropubic prostatectomy in the medicare population. *Urology* 2000; **56**: 116–20.

Supplementary materials

The following supplementary material is available for this article:

Fig. S1. The cell number of > G_2/M fractions decreased between 34 and 36 h. From the data sets presented in Figure 6a, the cell number of > G_2/M fractions was counted between 24 and 38 h using flow cytometry.

Fig. S2. Disappearance of large cells between 34 and 36 h. (A) From flow cytometry data sets, the aneuploid cell (A) and large-cell (L) populations were extracted, as described elsewhere. (B) From the data sets presented in (A), each cell population was monitored between 34 and 36 h.

This material is available as part of the online article from:
http://www.blackwell-synergy.com/doi/abs/10.1111/j.1349-7006.2008.00781.x

This link will take you to the article abstract).

Please note: Blackwell Publishing are not responsible for the content or functionality of any supplementary materials supplied by the authors. Any queries (other than missing material) should be directed to the corresponding author for the article.

doi: 10.1111/j.1349-7006.2008.00781.x

OPEN ACCESS Freely available online

PLoS one

The Anti-Proliferative Effects of the CHFR Depend on the Forkhead Associated Domain, but not E3 Ligase Activity Mediated by Ring Finger Domain

Tomokazu Fukuda, Yasuyuki Kondo, Hitoshi Nakagama*

Biochemistry Division, National Cancer Center Research Institute, Tokyo, Japan

Abstract

The CHFR protein comprises fork head associated- (FHA) and RING-finger (RF) domain and is frequently downregulated in human colon and gastric cancers up to 50%. The loss of CHFR mRNA expression is a consequence of promoter methylation, suggesting a tumor suppressor role for this gene in gastrointestinal carcinogenesis. In terms of the biological functions of CHFR, it has been shown to activate cell cycle checkpoint when cells are treated with microtubule depolymerizing agents. Furthermore, CHFR was reported to have E3 ligase activity and promote ubiquitination and degradation of oncogenic proteins such as Aurora A and polo-like kinase 1. However, molecular pathways involved in the tumor suppressive function of CHFR are not yet clear since the two established roles of this protein are likely to inhibit cell growth. In this study, we have identified that the FHA domain of CHFR protein is critical for growth suppressive properties, whereas the RF and cysteine rich domains (Cys) are not required for this function. In contrast, the RF and Cys domains are essential for E3 ligase activity of CHFR. By the use of a cell cycle checkpoint assay, we also confirmed that the FHA domain of CHFR plays an important role in initiating a cell cycle arrest at G2/M, indicating a functional link exists between the anti-proliferative effects and checkpoint function of this tumor suppressor protein via this domain. Collectively, our data show that the checkpoint function of the FHA domain of CHFR is a core component of anti-proliferative properties against the gastrointestinal carcinogenesis.

Citation: Fukuda T, Kondo Y, Nakagama H (2008) The Anti-Proliferative Effects of the CHFR Depend on the Forkhead Associated Domain, but not E3 Ligase Activity Mediated by Ring Finger Domain. PLoS ONE 3(3): e1776. doi:10.1371/journal.pone.0001776

Editor: Edathara Abraham, University of Arkansas, United States of America

Received January 28, 2008; **Accepted** February 12, 2008; **Published** March 12, 2008

Funding: This work was supported in part by a Grant-in-Aid for Cancer Research for the Third-Term Comprehensive 10-Year Strategy for Cancer Control from the Ministry of Health, Labour and Welfare of Japan, and by a Research Grant of the Sankyo Foundation of Life Science (06-016). Y.K. is a recipient of a Research Resident Fellowship from the Foundation for the Promotion of Cancer Research in Japan.

Competing Interests: The authors have declared that no competing interests exist.

* E-mail: hnakagam@gan2.res.ncc.go.jp

Introduction

CHFR (Checkpoint protein with Forkhead associated and Ring finger domain) was first isolated by a homology screening of EST cDNA clones harboring an FHA domain [1]. The CHFR protein is characterized by the existence of two domain structures that are well conserved across different species, namely the FHA and RING finger domains (RF) [1]. CHFR is in fact the only protein in vertebrates that contains both of these functional domains.

The FHA domain of CHFR has been reported to arrest the cell cycle under mitotic stress conditions caused by microtubule depolymerizing agents such as nocodazole, and this moiety thus confers a mitotic checkpoint function upon this protein [2–6]. In terms of the mechanisms underlying this checkpoint function, CHFR has been shown to exclude Cyclin B1 from the nucleus, resulting in the arrest of the cell cycle at around the G2 phase [7]. Other checkpoint regulators with an FHA domain, such as CHK2 and NBS1, have also shown similar features and arrest the cell cycle in response to DNA damage and replication blocks [8,9].

These checkpoint proteins containing FHA domain have been shown to function as tumor suppressors, although the detailed molecular mechanisms are not yet fully elucidated. For example, the inactivation of the CHK2 and NBS1 proteins increases the predisposition of cells to cancer development [8,10–14]. The functional inactivation of CHFR due to promoter methylation and the consequent loss of mRNA expression is frequently observed in human colon and gastric cancers [4,15–19], suggesting its possible role also as a tumor suppressor. The functional loss of these checkpoint proteins is likely to disrupt the cell cycle arrest response to cellular stress, thus leading to the accumulation of mutations and replication errors in the genome, a prerequisite for malignant transformation.

The RING-finger domain is a characteristic feature of the E3 ligase proteins [1] and is thought to determine the substrate specificity for ubiquitination reactions. As an example, the RING-finger protein cdc20 is known to serve as an E3 ligase for the anaphase promoting complex/cyclosome (APC/C) [20], and Cyclin B is also one of its substrates [20]. Cyclin B proteins that have been polyubiquitinated by cdc20 are rapidly transferred to the proteasome and degraded. CHFR was shown to play a role as E3 ligase for the polyubiqutination of Aurora A and Polo-like-kinase 1 [21,22], possibly resulting in the degradation of these proteins. In fact, mouse embryonic fibroblasts (MEF) derived from *Chfr* knockout mice show elevated protein levels of Aurora A and display chromosome abnormalities [21]. The inactivation of CHFR may thus cause the up-regulation of these proteins, which are known mitotic kinases and are frequently observed to be overexpressed in various types of human malignant tumors, such as bladder and colon cancers [23,24]. Elevated levels of Aurora A and Plk1 are known to induce abnormal mitotic cell division and

cause karyotype abnormalities or malignant transformation [25,26]. The functional loss of CHFR could therefore result in the accumulation of oncogenic proteins (Aurora A and Plk1) and induce genomic instability.

To date, two possible molecular pathways have been considered as the mechanisms underlying the tumor suppressor function of CHFR. These are the checkpoint regulation and E3 ligase functions of this protein. However, it is difficult to draw any conclusions from the findings of previous studies about which of these roles is the most critical for growth suppression, since functional analyses of the checkpoint and E3 ligase activity of CHFR have only been performed independently of each other thus far [1,22,27–29]. We initially focused on the E3 ligase activity as a possible pathway for the growth suppressive properties of CHFR as our previous data have shown that degradation by the proteasome is the major rate limiting step in the control of the Aurora A protein levels [30]. If the E3 ligase activity of CHFR is more important for growth suppression, as we initially expected, the core region of this tumor suppressor that is required for its anti-proliferative effects was anticipated to be the RF domain.

In our current study, we have investigated the molecular pathways underlying the growth suppressive functions of CHFR by utilizing genetic rescue experiments with colon cancer cell lines in which endogenous CHFR is epigenetically inactivated.

Materials and Methods

CHFR plasmids

A cDNA fragment of human CHFR (NIH Mammalian Gene Collection ID: 19963) was obtained by RT-PCR from a human pancreatic cancer cell line (Panc1) based on a method described previously [30]. A hemagglutinin (HA) protein tag sequence was then introduced at the amino terminus of this recombinant CHFR product and a Kozak sequence was inserted just upstream of the start codon of the HA protein tag. Mutant cDNA fragments were created using the quick change PCR kit (Stratagene) with slight modifications [31]. To generate a *Δ*FHA mutant, a CHFR cDNA fragment was generated that lacked the 110 amino acids between the original start methionine and the end of the FHA domain (MERPEEGKQS-EPEHNVAYLYESLS). An RF mutant (*Δ*RF) was similarly designed by generating a truncated CHFR cDNA lacking this 48 amino acid domain (CIICQDLLHD-TCRCPVERICK). A TGA stop codon was inserted into the CHFR cDNA to construct the cysteine rich domain mutant (*Δ*Cys) by producing a protein product lacking the 190 amino acids of this region (VCPLQGSHAL-HICEQTRFKN).

Each cDNA was subcloned into the EcoRV site of pBluescript SKII+ (Stratagene) by blunt end ligation, and the resulting constructs were validated in a cycle sequencing reaction with an ABI 310 genetic analyzer (Applied Biosystems). Both the wild-type and mutant CHFR cDNA fragments were also subcloned into an LXIN retrovirus vector (Clontech), the pcDNA 3.1+ plasmid (Invitrogen), and an IRES2-EGFP bicistronic expression vector (Clontech). The retrovirus vectors were used in colony formation assays, whereas the pcDNA 3.1+ vectors were used in an *in vivo* ubiquitination assay and also in the cellular localization experiments. The bicistronic vectors (IRES2-EGFP) were employed in the checkpoint analyses.

Stable and transient expression of wild-type and mutant CHFR proteins in cultured cells

HCT116, RKO and HeLa cells were cultured in Dulbecco's Modified Eagle's Medium (DMEM; Sigma) supplemented with 10% fetal bovine serum (FBS), penicillin (100U/ml), and streptomycin (50U/ml), at 37°C and 5% CO_2. A PT67 retrovirus packaging cell line was obtained from Clontech, and maintained in DMEM with 10% FBS. Cells were maintained in an exponential growth phase prior to use.

Retroviral constructs harboring wild-type or mutant human *CHFR* cDNAs, were introduced into PT67 cells (Clontech) for packaging using the lipofection method (Fugene 6, Roche). The LXIN retroviral vector contains a neomycin cassette, and cells that stably produced recombinant retroviruses were selected after two weeks of culture in the presence of 1 mg/ml G418. The retroviral supernatants were diluted 1:2 with normal DMEM containing 10% FBS and exposed to HCT116 or RKO cells with 400 μg/ml of polybrane infection enhancer. Infected cells were further selected with 1 mg/ml G418 for two weeks. To avoid cloning bias, the whole cell population that showed resistance to G418 was used in each experiment. For transient expression experiments, cells at 70% confluency were transfected with 2.5 μg of the indicated plasmids using the lipofection method (Lipofectamine 2000, Invitrogen), according to the manufacturer's protocol.

Colony formation assay

1×10^6 HCT116, RKO or HeLa cells were infected with aliquots of LXIN retroviral supernatants from the PT67 packaging cells for 48 h. When the infected cells reached confluence, they were trypsinized and resuspended in 10 ml of DMEM supplemented with 10% FBS. 10 μl (HCT116) or 100 μl (RKO or HeLa) aliquots of these cell suspensions were then seeded into 100 mm culture dishes (Nunc, 150350), and grown in G418 selection for two weeks as described above. G418-resistant colonies were subsequently fixed in 4% paraformaldehyde in phosphate buffered saline (PBS), and stained with hematoxilin. Images of the stained dishes were captured using a high-resolution digital camera with a macro lens (Fuji Film), and the numbers of colonies were determined in each image using NIH image software. The average colony numbers were then calculated from five dishes in three independent experiments. Statistical significance was evaluated with the Wilcoxon-Mann-Whitney *U*-test.

Measurement of the retrovirus titers of the producer cells

The conditioned medium of the producer cells was diluted 1:50 with distilled water and subjected to reverse transcription. The copy number of the resulting retroviral cDNA was measured by real-time PCR with a Retrovirus titer set (Takara Bio, Kyoto, Japan). The average retrovirus copy number of per ml was determined from five independent reactions. The reverse transcriptase and real-time PCR reactions were performed according to the manufacturer's instructions.

Western blot analysis

Cells were lysed in ice-cold HIPS buffer (50 mM Tris-HCl, pH 7.5, 150 mM NaCl, 1% Triton X-100) [30] and the resulting whole cell lysates were subjected to 10% SDS-PAGE. The separated proteins were then transferred to polyvinylidene difluoride (PVDF) membranes (Immobilon P, Millipore). After blocking with 7% non-fat dry milk-Tris buffered saline and 0.1% Tween 20 (TBST), the membranes were probed with anti-HA (High affinity HA 3F10, 1/5,000 dilution, Roche), and anti-α-tubulin (DM-1A, 1/5,000 dilution, ICN Biomedicals) antibodies. Blots were then incubated with horseradish peroxidase (HRP)-conjugated rabbit anti-rat IgG (A5795, 1/5,000 dilution, Roche) or donkey anti-mouse IgG (NA1093V, 1/5,000 dilution, GE Healthcare Bioscience) secondary antibodies respectively, and immunoreactive proteins were detected by enhanced chemiluminescence (P90720, Millipore).

In vivo ubiquitination assay

2.5 μg of wild-type and mutant CHFR pcDNA 3.1+ expression plasmids, and an empty vector control, were introduced into HCT116 cells at 70% confluency using the lipofection method (Lipofectamine 2000, Invitrogen). 2.5 μg of pcDNA 3.1+ vector harboring FLAG tagged ubiquitin (kindly provided by Dr. K. Miyazono, Tokyo University) was co-transfected with these constructs. After 20 h, the cells were treated with 25 μM of MG132 (C2211, SIGMA) for 5 h, lysed in HIPS buffer, and subjected to immunoprecipitation. A 500 μg aliquot of total protein from the transfected HCT116 cells in 250 μl lysis solution was mixed with 10 μl of the anti-HA affinity matrix (Roche) pre-blocked with 2% bovine serum albumin (BSA), and incubated for 4 h with gentle rotation at 4°C. The affinity matrix was washed with HIPS buffer three times, collected by centrifugation, and the precipitated proteins were denatured in sample buffer containing 0.1M dithiothreitol (DTT), subjected to 7% SDS-PAGE and transferred to a PVDF membrane. The transferred proteins were then incubated with anti-HA (high affinity HA 3F10, 1/5,000 dilution, Roche), or anti-FLAG (monoclonal anti-FLAG M2, 1/5,000 dilution, Sigma) antibodies. The secondary antibodies used were as described above for the western blotting procedure.

Intracellular localization of CHFR protein

pcDNA3.1+ expression vectors were introduced into HCT116 cells using the lipofection method, as described earlier. Twenty-four hours after transfection, the cells were fixed with 4% paraformaldehyde and then treated with 0.5% Triton X-100 (both in PBS) for 5 min. The cells were preblocked with 1% normal goat serum (NGS) in PBS for 30 min and incubated with an anti-HA antibody (high affinity HA 3F10, 1:500 dilution, Roche) for 1 h at room temperature. An alexa 488-conjugated goat anti-rat IgG (Invitrogen) was used as the secondary antibody. A rabbit PML antibody (PM001, 1/300 dilution, MBL) and alexa 594-conjugated goat anti-rabbit IgG (Invitrogen) were used to detect PML nuclear foci. The cells were counter-stained in each case with 1μM of Hoechst 33258 (B1155, Sigma) and staining images were captured using an Axiovart (Zeiss) fluorescence microscope.

Cell cycle checkpoint analysis

For checkpoint analysis, HCT116 cells were transfected with IRES2-EGFP expression plasmids harboring wild-type or mutant CHFR inserts for 5 h and then treated with nocodazole at a concentration of 200 ng/ml (from a 100 mg/ml stock solution in dimethyl sulfoxide, Sigma) for 16 h. After the nocodazole treatment, the cells were fixed in 4% paraformaldehyde/PBS and the numbers of mitotic cells, which show EGFP fluorescence, were determined by microscopic examination. The average percentage of the total EGFP-positive cells that were deemed to be mitotic was calculated by counting approximately 100 cells expressing either wild-type or mutant CHFR proteins.

Results

The expression of wild-type and mutant CHFR proteins in colon cancer cells which lack the endogenous species

Colon cancer cells have lost the endogenous expression of CHFR, and we thus anticipated that this would be an appropriate cell system to elucidate the functional domain responsible for the anti-proliferative effects of CHFR protein by genetic rescue. The endogenous levels of *CHFR* mRNA were measured by real-time RT-PCR in five pancreatic cancer cell lines and six colon cancer cell lines (Fig. 1C). *CHFR* transcripts were detectable in each of the pancreas cell lines tested but three colon cancer derived cell lines, HCT116, RKO and DLD1, showed no expression of *CHFR* mRNA.

The structures of the wild-type and mutant CHFR proteins are shown in Figure 1A. Expression vectors for these proteins were introduced transiently into HCT116 cells and subjected to western blotting with anti-HA antibodies to determine whether the predicted recombinant CHFR proteins were produced (Fig. 1B). Positive bands were indeed detected at the expected molecular weights (wild-type; 72 kDa, ΔFHA; 57 kDa, ΔRF; 66 kDa, ΔCys; 50 kDa), indicating that each CHFR protein product was efficiently expressed.

The anti-proliferative effects of CHFR are dependent upon the FHA domain and not the RF or Cys domains

To evaluate the effects of wild-type and mutant CHFR proteins (ΔFHA, ΔRF and ΔCys) on cell proliferation, recombinant retroviruses harboring the corresponding cDNAs were introduced into HCT116 cells. There were no major differences found in the resulting cell morphologies in each case, as shown in Figure 2A. Substantial growth suppression was observed following the introduction of the wild-type CHFR during G418 selection (Fig. 2A). In addition, whereas the ΔRF and ΔCys mutants showed growth suppressive effects that were almost identical to the wild-type CHFR, the ΔFHA protein had minimal inhibitory effects upon cell proliferation (Fig. 2A).

To more quantitatively evaluate the growth inhibitory effects of the wild-type and mutant CHFR proteins, a colony formation assay was carried out using the corresponding retrovirally infected HCT116 cells under G418 selection (Fig. 2B and C). The expression of wild-type, ΔRF and ΔCys proteins resulted in a significant decrease in the number of G418-resistant colonies in this experiment compared with the vector control ($p<0.01$), whereas ΔFHA expressing cells did not show any reduction in colony number. The same recombinant *CHFR* retroviruses were also introduced into RKO cells and similar results were observed (Fig. 2C).

To verify the titer of our recombinant CHFR retroviruses, the virus copy numbers in the conditioned supernatant of the PT67 producer cells were measured by real-time PCR. As shown in Figure 2D, no major differences could be observed in the retrovirus copy number between the wild-type and mutant CHFR retrovirus producer cells. We therefore concluded that the growth suppressive effects of CHFR that we observed in these analyses are not due to any differences in the titers of the producer cells.

Detection of wild-type and mutant CHFR proteins under stable expression conditions

During their initial passages, significant growth suppression was observed in HCT116 cells expressing exogenous wild-type, ΔRF and ΔCys CHFR, as shown in Figures 2A–C. However, this growth suppression becomes almost undetectable by passage 3. The protein levels of each of these introduced CHFR products were thus analyzed in these cells at passage 4 by western blotting. As shown in Figure 2E, the levels of the wild-type, ΔRF and ΔCys products were remarkably low when compared with ΔFHA (Fig. 2E, left panel). The same analysis was undertaken in RKO cells and produced essentially identical results (Fig. 2E, right panel). A possible explanation for this phenomenon is that elevated levels of wild-type, ΔRF and ΔCys proteins may cause a substantial growth disadvantage, and thus cell populations which express these introduced proteins at low levels undergo positive selection with passage in culture.

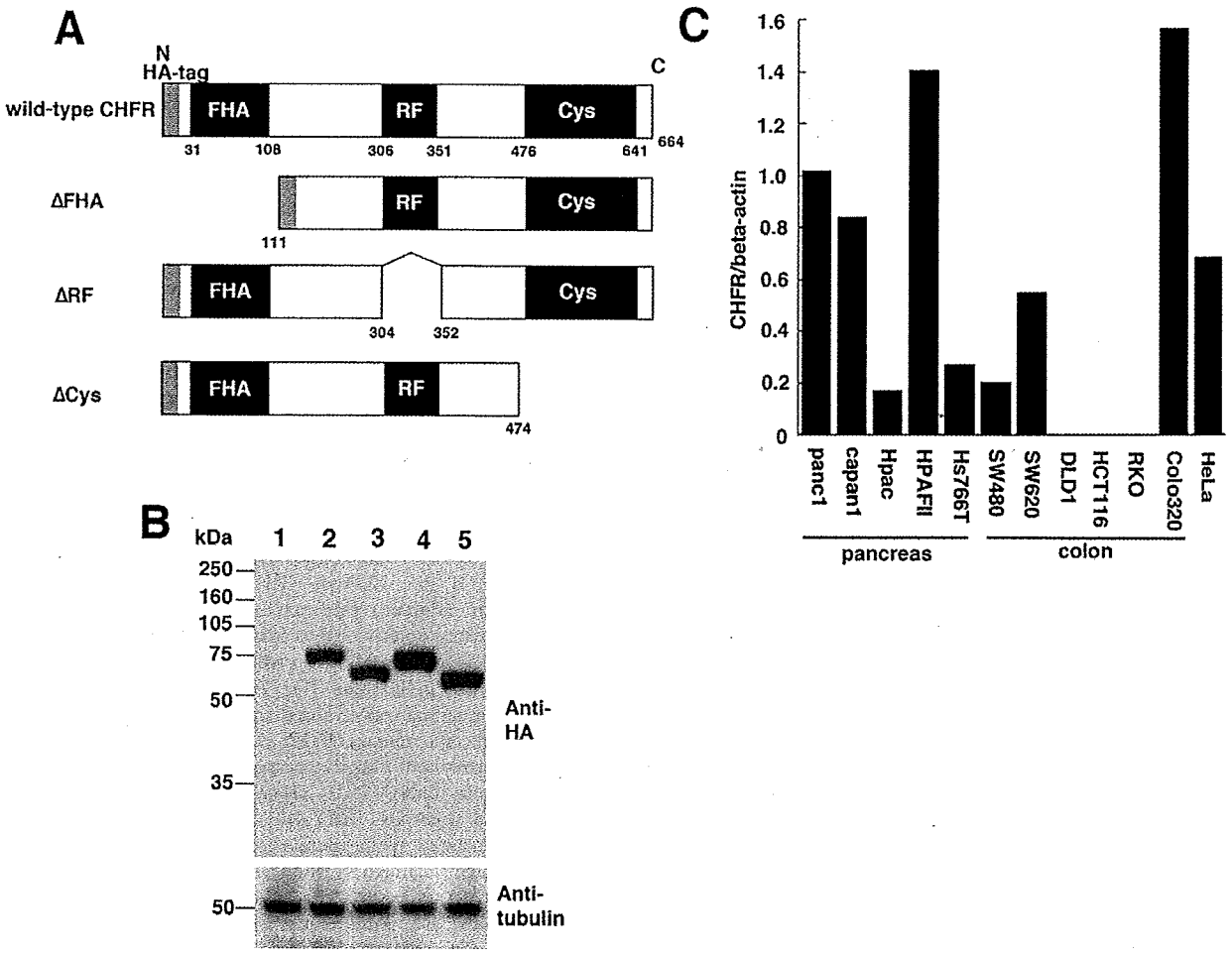

Figure 1. Schematic representation of the wild-type, ΔFHA, ΔRF and ΔCys forms of the CHFR protein tagged with HA, and expression analysis of these proteins in a colon cancer-derived cell line that lacks endogenous CHFR mRNA. (A) The predicted protein structures of the wild-type, ΔFHA, ΔRF and ΔCys CHFR proteins. N and C indicate the amino and carboxyl terminus, respectively. FHA, forkhead associated domain; RF, ring finger domain; Cys, cysteine rich domain; HA-tag, hemagglutinin protein tag. (B) The detection of the wild-type, ΔFHA, ΔRF and ΔCys forms of CHFR proteins transiently expressed in HCT116 cells by western blotting with anti-HA antibodies (upper panel). Cells were transfected with HA-tagged empty vector (lane 1); wild-type CHFR (lane 2); ΔFHA (lane 3); ΔRF (lane 4); or ΔCys (lane 5). Tubulin was also detected as a loading control (lower panel). (C) Endogenous CHFR mRNA expression levels detected by real-time PCR in the indicated pancreatic- and colon cancer-derived cell lines. The relative levels of CHFR mRNA shown are normalized to beta-actin mRNA, the expression level of panc1 was set as 1.0, and the average values of duplicate experiments were calculated.
doi:10.1371/journal.pone.0001776.g001

The E3 ligase activity of CHFR requires the RF and Cys domains, but not the FHA domain

A series of *in vivo* ubiquitination assays were conducted using HCT116 cell populations that transiently expressed the wild-type and mutant CHFR proteins at similar levels (Fig 3, left panel). The recombinant CHFR and its substrate proteins were immunoprecipitated from the corresponding cellular extracts with an anti-HA antibody and the ubiquitination activity levels were then monitored by western analysis with anti-FLAG antibodies to detect high molecular weight bands as described in a previous study [32]. As shown in the right panel of Figure 3, polyubiquitinated proteins were detectable in cells expressing wild-type and ΔFHA proteins but not the ΔRF and ΔCys mutants, which is deemed to be substrates of CHFR. The mobilities of these immunoprecipitated CHFR proteins were also not altered as a result of polyubiquitination (Fig. 3, middle panel), indicating that no self-ubiquitination had occurred in each case. From these results, we concluded that E3 ligase activity of CHFR requires the RF and Cys domains, but is unaffected by the deletion of the FHA domain.

Analysis of the intracellular localization of wild type, ΔFHA, ΔRF and ΔCys CHFR proteins by immunofluorescence staining

A previous study has indicated that the FHA domain of the CHFR protein is essential for its localization in promyelocytic leukemia (PML) foci within the nucleus [33]. The intracellular localization of the wild type and mutant CHFR proteins was detected by immunostaining of HCT116 cells that exogenously expressed these products. As shown in Figure 4, each of these

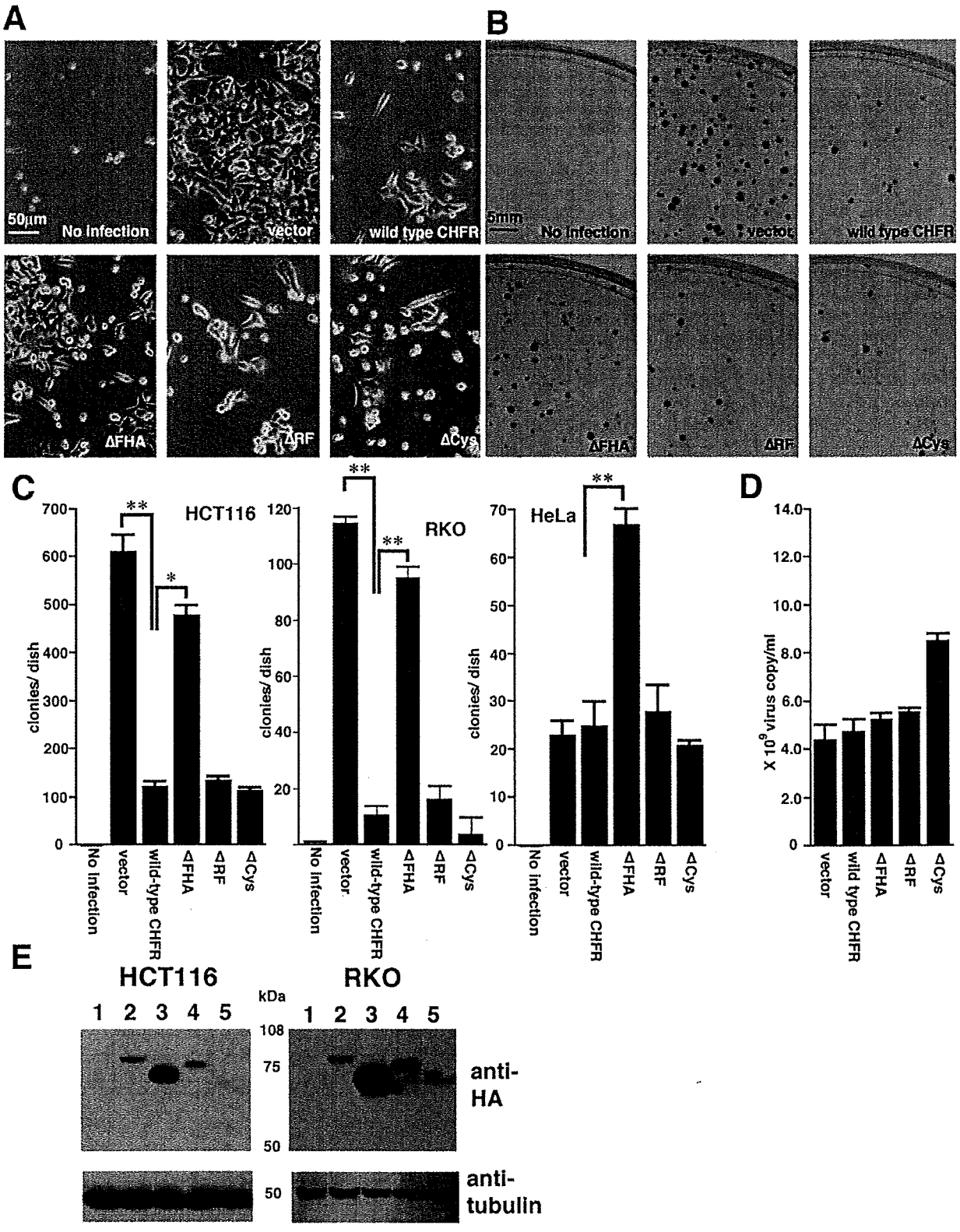

Figure 2. Identification of the functional domain of the CHFR protein that confers its anti-proliferative effects. (A) The growth appearance of HCT116 cells infected with retroviral vectors expressing the indicated CHFR products. Note that the wild-type CHFR, ΔRF and ΔCys retroviruses suppressed the cell growth of the host cells and this was partially restored in the ΔFHA expressing cells. There were no differences,

←

however, between any of these transfected cells in terms of their morphology. (B) Colony formation assay of HCT116 cells after retroviral infection with the same CHFR constructs as in (A). (C) Statistical evaluation of the colony formation assay results for HCT116, RKO and HeLa cells expressing the indicated exogenous proteins. *p<0.01, **p<0.05. (D) Measurements of the recombinant retrovirus copy number in the supernatants of PT67 producer cells by real time PCR. (E) The detection of stably expressed wild-type, ΔFHA, a ΔRF and ΔCys CHFR protein in HCT116 and RKO cells following infection with the corresponding recombinant retroviruses. Total cellular protein extracts were obtained at the fourth passage. The level of introduced proteins in the cells that infected with empty vector (lane 1); wild-type CHFR (lane 2); ΔFHA (lane 3); ΔRF (lane 4); or ΔCys (lane 5).
doi:10.1371/journal.pone.0001776.g002

introduced CHFR species showed a diffuse nuclear localization and no differences could be observed. Although the cells were doubly stained with anti-HA and anti-PML antibodies, a dominant accumulation of CHFR within the PML nuclear foci was not evident for either the wild type or mutant proteins. From these data, we conclude that the CHFR domains analyzed do not impact upon the intracellular localization of this protein.

The checkpoint function of CHFR requires the FHA domain only

The functional recovery of the checkpoint function of CHFR was evaluated also in HCT116 cells after the exogenous introduction of wild type and mutant CHFR proteins. Since the transfection efficiency was limited to around 5% for the transient expression vector, a bicistronic expression vector harboring the CHFR wild type and mutant inserts was used in these experiments (Fig. 5A). Since in this case the CHFR and EGFP protein products are translated from the same mRNA, EGFP fluorescence can be used as a marker of recombinant CHFR protein expression. To validate the positive correlation between EGFP expression and CHFR expression, the percentage of EGFP positive cells that were immunoreactive also for the anti-HA antibody was determined microscopically (Fig 5B). Among the 200 EGFP-positive cells that were counted, 182 (91%) showed positive staining for anti-HA antibody (Fig. 5B), confirming the usefulness of EGFP as a marker. As shown in Figure 5C, following nocodazole treatment, the percentage of EGFP-positive mitotic cells was found to decrease in conjunction with the expression of the wild type, ΔRF and ΔCys CHFR proteins, compared with the vector control. In contrast, the expression of the ΔFHA mutant did not affect the percentage of mitotic cells. From these data, we conclude that the FHA domain is essential for the mitotic checkpoint function of CHFR.

Discussion

Our current study has identified the CHFR domains that are responsible for the anti-proliferative effects of this protein and the results are summarized in Table 1. We find that both the anti-proliferative effects and checkpoint function of CHFR require the FHA domain, whereas the E3 ligase activity of this tumor suppressor relies on the RF and Cys domains. This suggests that there is a functional link between the anti-proliferative effects and checkpoint function of CHFR. Our present analyses also reveal that the FHA domain is the most important region of CHFR for its anti-proliferative role, which is in good agreement with several previous studies. Toyota *et al* have also reported that the introduction of a wild-type CHFR expression vector causes the growth suppression of the host cells, whereas a FHA deletion mutant did not affect cell growth [19].

Although the data presented by Toyota *et al* was quite suggestive of the essential role of FHA in cell growth control, it should be noted that the cell lines they analyzed (SW480 and T98G) endogenously express CHFR transcripts (see Fig. 1C for SW480) [34]. The accurate and quantitative evaluation of the impact of the ΔFHA mutant on cell growth is difficult to undertake in the presence of endogenous protein because of the dominant-negative properties of this mutant [1]. Interestingly, we detected that the expression of these mutant CHFR proteins had a completely different result upon the growth of HeLa cells, which express

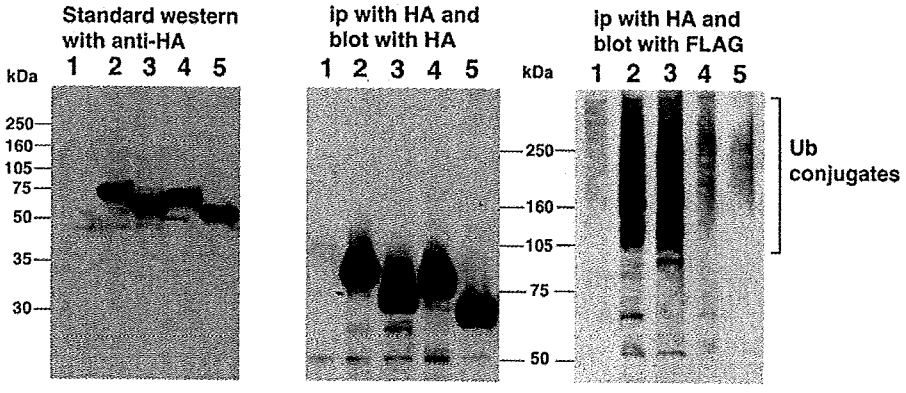

Figure 3. *In vivo* ubiquitination assay for the wild-type, ΔFHA, ΔRF and ΔCys forms of the CHFR protein. (Left panel) Measurement of the transient expression levels of both the wild-type and mutant form of CHFR proteins in HCT116 cells by western blotting. The proteins were separated by 10% SDS-PAGE. (Middle panel) Immunoprecipitation and immunoblotting of proteins with anti-HA antibodies. The proteins were resolved by 7.5% SDS-PAGE. (Right panel) The detection of FLAG-reactive proteins following immunoprecipitation by HA antibodies. Ubiquitinated proteins are evident by the presence of high molecular weight bands in lanes 2 and 3, but not in lanes 1, 4 and 5. Cells were cotransfected with FLAG tagged ubiquitin expression (FLAG-Ubi) vector and either empty vector (lane 1); wild-type CHFR (lane 2); ΔFHA (lane 3); ΔRF (lane 4); or ΔCys (lane 5).
doi:10.1371/journal.pone.0001776.g003

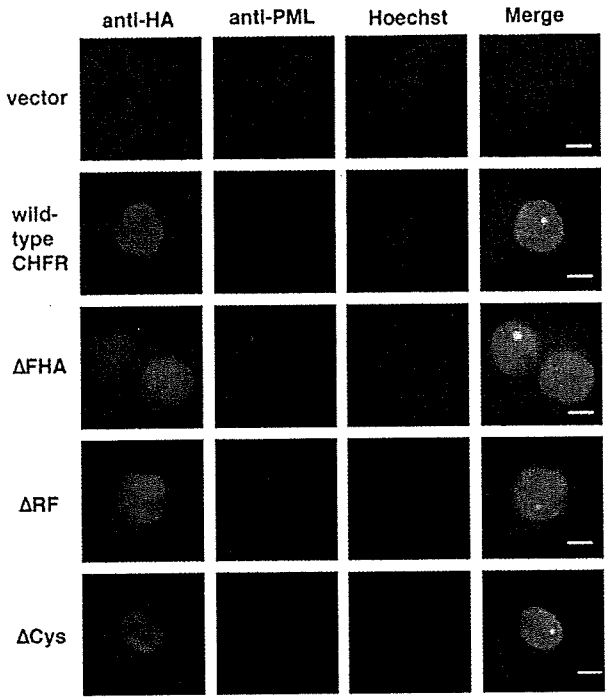

Figure 4. Intracellular localization of wild-type and mutant forms of CHFR proteins detected by fluorescence immunostaining. The localization of the wild-type or mutant forms of the CHFR protein was assessed by the immunoreactivity of an anti-HA antibody (green signal). PML nuclear foci were detected with an anti-PML antibody (red signal). The nuclei of HCT116 cells were counterstained with Hoechst (blue). Merged pictures are shown to highlight the signal overlap between the Hoechst and anti-HA staining.
doi:10.1371/journal.pone.0001776.g004

endogenous CHFR, compared with HCT116 and RKO cells (Fig. 2C). In these experiments, the expression of ΔFHA induced a significant increase in colony number whereas the wild-type, ΔRF and ΔCys CHFR species did not show any effects (Fig. 2C, Right panel). A previous study has indicated that the ΔFHA mutant of CHFR acts as a dominant-negative and can disrupt the checkpoint function of the wild type protein [1]. Hence, we speculated that the increase in the colony number in HeLa cells by ΔFHA was caused by the dominant-negative effects of this mutant upon the endogenous wild type CHFR protein [1]. The reported existence of a splicing variant form of CHFR that lacks the FHA domain and acts in a dominant-negative manner further supports our contention [19]. It has not yet been reported until this manuscript to evaluate the effect of FHA domain against cell proliferation under the two conditions, the existence and non-existence of endogenous CHFR. We therefore conclude that our current study is the first report that precisely identifies the functional domain responsible for the anti-proliferative function of CHFR.

We show from our analysis that the loss of the RF domain and its associated E3 ligase activity did not disrupt the anti-proliferative effects of CHFR, suggesting that the E3 ligase activity of this protein is not essential for its tumor suppressor function. From previous functional analysis of CHFR knockout mice, however, Yu *et al* concluded that the tumor suppressor function of CHFR is conferred by its E3 ligase activity toward the Aurora A protein, a predicted oncogenic kinase [21]. There is therefore some disagreement regarding the precise role of the E3 ligase activity of CHFR, but possible explanation can be considered. We need to pay attention to the tissue specificity of CHFR to induce the degradation of Aurora A. Elevated protein levels of Aurora A are frequently observed in both human colon and mammary cancers [25,26], but the inactivation of CHFR is limited to cases of colon cancer [17,35]. High levels of Aurora A in mammary cancers cannot therefore be explained by a loss of function of CHFR. These findings indicate the existence of degradation pathways for Aurora A that are independent of CHFR [17]. In this regard, Cdh1 is a strong candidate as an alternative E3 ligase for Aurora A [36,37]. The exogenous introduction of a dominant-negative form of Cdh1 was reported to induce elevated levels of Aurora A protein in HeLa cells [37]. Hence, there may be several molecular pathways that promote the degradation of Aurora A but that are tissue- or organ-specific. The protein levels of Aurora A did not change after the expression of any form of CHFR in HCT116 colon cancer cells in our current experiments (data not shown). The differences between the findings of this and other studies might thus be due to the cell-type specificity of the degradation pathways for Aurora A.

With regards to the E3 ligase activity of CHFR, we found that the RF and Cys domains are essential. These results are consistent with previously reported findings, which show that CHFR binds to its substrates through its Cys domain, and forms a protein complex with APC/C through its RF domain [21]. Some E3 ligases have also been reported to have self-ubiquitination activity [38,39], but we did not detect this in the case of CHFR. In contrast, Kang *et al* have reported strong self-ubiquitination activity for CHFR [22]. One possibility to be taken into consideration when evaluating these discrepancies is the difference of their GST protein tag and our HA tag. The self ubiquitination activity affected by the protein tag has reported with MBP protein tag in case of Rma1, EL5 and Perkin [40–42]. Therefore, further experiments with other protein tags would be needed to get the conclusion about the self ubiquitination activity of CHFR protein.

The results of our current study also show that the expression of CHFR arrests the cell cycle prior to entry into mitosis in the presence of microtubule depolymerizing reagents, which is consistent with previous reports [1,19,22,27,28]. A growth advantage will be conferred upon cells which have lost the checkpoint machinery that functions under mitotic stress conditions. In agreement with this idea, shRNA knock down of CHFR recently reported to induce the increased cell proliferation during the preparation of this manuscript [43]. Since the promoter methylation of the *CHFR* gene was detected in non-invasive adenoma lesions of colon epithelia [44], the associated loss of the checkpoint function of CHFR in these cells may have a significant impact upon the early stages of colon carcinogenesis. To gain further supportive evidence that the FHA domain of CHFR is important for its growth inhibition properties, we have recently put a considerable amount of effort into establishing a conditional expression system for this protein using the Cre-loxP recombination system [30] to evaluate tumor formation activity *in vivo* (e.g. nude mice). Unfortunately, we have yet to establish an efficient conditional system due to the toxicity of Cre-expressing adenovirus in HCT116 colon cancer cells. Although it is not direct evidence, a remarkably high protein level of the ΔFHA mutant, compared with that of the wild-type and other mutant forms of CHFR, suggests that the FHA domain has an important role in suppressing tumor formation (Fig. 2E). The FHA domain is expected to work as the binding motif for phosphorylated proteins. We are currently working on the experiments to isolate the binding partner of FHA domain of CHFR protein. There is a possibility that the detail of anti-

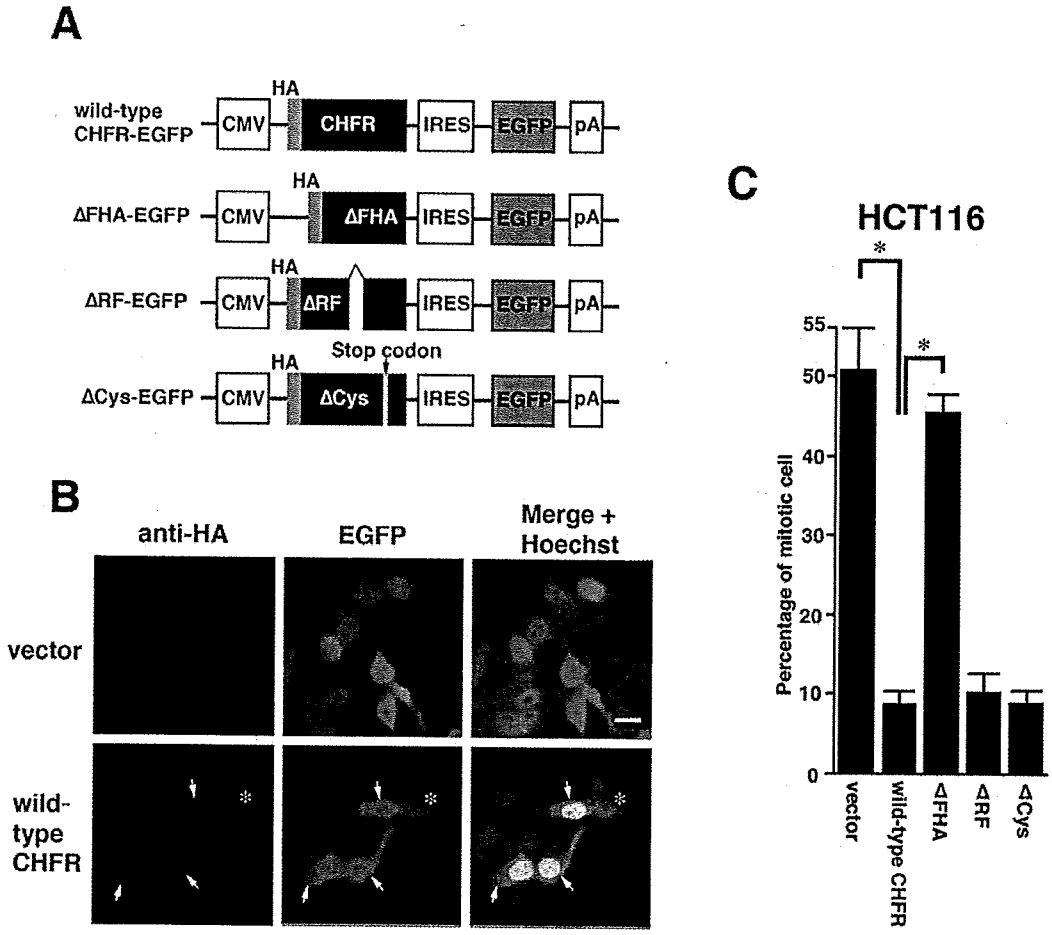

Figure 5. Checkpoint assay of the wild type and mutant forms of the CHFR protein. (A) Schematic representation of the bicistronic vectors used to express the indicated CHFR products. (B) Validation of the positive correlation between the anti-HA antibody immunoreactivity and EGFP expression profiles. Cells that were positive for both are denoted by arrows. Cells that were positive for the anti-HA antibody, but not for EGFP, are highlighted by an asterisk. (C) Mitotic checkpoint analysis of HCT116 cells after the introduction of an empty vector, wild-type-EGFP, ΔFHA-EGFP, ΔRF-EGFP or ΔCys-EGFP. Asterisks indicate statistical significance ($p<0.05$).
doi:10.1371/journal.pone.0001776.g005

proliferative effect can be explained with the binding of new candidates and CHFR. These information will help us to gain further insights in understanding how a functional loss of this gene leads to increased cell proliferation during gastrointestinal carcinogenesis.

Table 1. Summary of the functional properties of wild-type, ΔFHA, ΔRF and ΔCys CHFR proteins.

	Wild type CHFR	ΔFHA	ΔRF	ΔCys
Anti-proliferative effects	Yes	No	Yes	Yes
E3 ligase activity	Yes	Yes	No	No
Cellular localization	Nucleus	Nucleus	Nucleus	Nucleus
Checkpoint function	Yes	No	Yes	Yes

doi:10.1371/journal.pone.0001776.t001

Acknowledgments

We thank Noriyuki Matsuda and Yukiko Yoshida (Tokyo Metropolitan Institute of Medical Sciences, Tokyo, Japan), Mitsuyasu Kato and Hiroyuki Suzuki (University of Tsukuba, Institute of Basic Medical Sciences) for their helpful advice and discussions, providing the FLAG-Ubiquitin expression plasmid. We also thank Hiroshi Tazawa, Naoto Tsuchiya, Daisuke Maeda and Tasuku Suzuki (Biochemistry Division and ADP-ribosylation in Oncology project in the National Cancer Center Research Institute) for technical help and discussions throughout this study. We are grateful to Hideko Fukuda (National Institute of Environmental Health Studies, Tsukuba, Japan) for her support and encouragement throughout this project.

Author Contributions

Conceived and designed the experiments: TF. Performed the experiments: TF YK. Analyzed the data: TF YK. Contributed reagents/materials/analysis tools: TF. Wrote the paper: TF. Other: Supervised the experiments and study: HN.

References

1. Scolnick DM, Halazonetis TD (2000) Chfr defines a mitotic stress checkpoint that delays entry into metaphase. Nature 406: 430–435.
2. Hamilton JP, Sato F, Greenwald BD, Suntharalingam M, Krasna MJ, et al. (2006) Promoter methylation and response to chemotherapy and radiation in esophageal cancer. Clin Gastroenterol Hepatol 4: 701–708.
3. Koga Y, Kitajima Y, Miyoshi A, Sato K, Sato S, et al. (2006) The significance of aberrant CHFR methylation for clinical response to microtubule inhibitors in gastric cancer. J Gastroenterol 41: 133–139.
4. Satoh A, Toyota M, Itoh F, Sasaki Y, Suzuki H, et al. (2003) Epigenetic inactivation of CHFR and sensitivity to microtubule inhibitors in gastric cancer. Cancer Res 63: 8606–8613.
5. Yanokura M, Banno K, Kawaguchi M, Hirao N, Hirasawa A, et al. (2007) Relationship of aberrant DNA hypermethylation of CHFR with sensitivity to taxanes in endometrial cancer. Oncol Rep 17: 41–48.
6. Yoshida K, Hamai Y, Suzuki T, Sanada Y, Oue N, et al. (2006) DNA methylation of CHFR is not a predictor of the response to docetaxel and paclitaxel in advanced and recurrent gastric cancer. Anticancer Res 26: 49–54.
7. Summers MK, Bothos J, Halazonetis TD (2005) The CHFR mitotic checkpoint protein delays cell cycle progression by excluding Cyclin B1 from the nucleus. Oncogene 24: 2589–2598.
8. Dasika GK, Lin SC, Zhao S, Sung P, Tomkinson A, et al. (1999) DNA damage-induced cell cycle checkpoints and DNA strand break repair in development and tumorigenesis. Oncogene 18: 7883–7899.
9. Durocher D, Jackson SP (2002) The FHA domain. FEBS Lett 513: 58–66.
10. Williams BR, Mirzoeva OK, Morgan WF, Lin J, Dunnick W, et al. (2002) A murine model of Nijmegen breakage syndrome. Curr Biol 12: 648–653.
11. Jongmans W, Vuillaume M, Chrzanowska K, Smeets D, Sperling K, et al. (1997) Nijmegen breakage syndrome cells fail to induce the p53-mediated DNA damage response following exposure to ionizing radiation. Mol Cell Biol 17: 5016–5022.
12. Vahteristo P, Tamminen A, Karvinen P, Eerola H, Eklund C, et al. (2001) p53, CHK2, and CHK1 genes in Finnish families with Li-Fraumeni syndrome: further evidence of CHK2 in inherited cancer predisposition. Cancer Res 61: 5718–5722.
13. Hirao A, Cheung A, Duncan G, Girard PM, Elia AJ, et al. (2002) Chk2 is a tumor suppressor that regulates apoptosis in both an ataxia telangiectasia mutated (ATM)-dependent and an ATM-independent manner. Mol Cell Biol 22: 6521–6532.
14. Takai H, Naka K, Okada Y, Watanabe M, Harada N, et al. (2002) Chk2-deficient mice exhibit radioresistance and defective p53-mediated transcription. Embo J 21: 5195–5205.
15. Brandes JC, van Engeland M, Wouters KA, Weijenberg MP, Herman JG (2005) CHFR promoter hypermethylation in colon cancer correlates with the microsatellite instability phenotype. Carcinogenesis 26: 1152–1156.
16. Homma N, Tamura G, Honda T, Jin Z, Ohmura K, et al. (2005) Hypermethylation of Chfr and hMLH1 in gastric noninvasive and early invasive neoplasias. Virchows Arch 446: 120–126.
17. Bertholon J, Wang Q, Falette N, Verny C, Auclair J, et al. (2003) Chfr inactivation is not associated to chromosomal instability in colon cancers. Oncogene 22: 8956–8960.
18. Corn PG, Summers MK, Fogt F, Virmani AK, Gazdar AF, et al. (2003) Frequent hypermethylation of the 5′ CpG island of the mitotic stress checkpoint gene Chfr in colorectal and non-small cell lung cancer. Carcinogenesis 24: 47–51.
19. Toyota M, Sasaki Y, Satoh A, Ogi K, Kikuchi T, et al. (2003) Epigenetic inactivation of CHFR in human tumors. Proc Natl Acad Sci U S A 100: 7818–7823.
20. Visintin R, Prinz S, Amon A (1997) CDC20 and CDH1: a family of substrate-specific activators of APC-dependent proteolysis. Science 278: 460–463.
21. Yu X, Minter-Dykhouse K, Malureanu L, Zhao WM, Zhang D, et al. (2005) Chfr is required for tumor suppression and Aurora A regulation. Nat Genet 37: 401–406.
22. Kang D, Chen J, Wong J, Fang G (2002) The checkpoint protein Chfr is a ligase that ubiquitinates Plk1 and inhibits Cdc2 at the G2 to M transition. J Cell Biol 156: 249–259.
23. Strebhardt K, Ullrich A (2006) Targeting polo-like kinase 1 for cancer therapy. Nat Rev Cancer 6: 321–330.
24. Nigg EA (2001) Mitotic kinases as regulators of cell division and its checkpoints. Nat Rev Mol Cell Biol 2: 21–32.
25. Bischoff JR, Anderson L, Zhu Y, Mossie K, Ng L, et al. (1998) A homologue of Drosophila aurora kinase is oncogenic and amplified in human colorectal cancers. Embo J 17: 3052–3065.
26. Zhou H, Kuang J, Zhong L, Kuo WL, Gray JW, et al. (1998) Tumour amplified kinase STK15/BTAK induces centrosome amplification, aneuploidy and transformation. Nat Genet 20: 189–193.
27. Ogi K, Toyota M, Mita H, Satoh A, Kashima L, et al. (2005) Small interfering RNA-induced CHFR silencing sensitizes oral squamous cell cancer cells to microtubule inhibitors. Cancer Biol Ther 4: 773–780.
28. Chaturvedi P, Sudakin V, Bobiak ML, Fisher PW, Mattern MR, et al. (2002) Chfr regulates a mitotic stress pathway through its RING-finger domain with ubiquitin ligase activity. Cancer Res 62: 1797–1801.
29. Bothos J, Summers MK, Venere M, Scolnick DM, Halazonetis TD (2003) The Chfr mitotic checkpoint protein functions with Ubc13-Mms2 to form Lys63-linked polyubiquitin chains. Oncogene 22: 7101–7107.
30. Fukuda T, Mishina Y, Walker MP, DiAugustine RP (2005) Conditional transgenic system for mouse aurora a kinase: degradation by the ubiquitin proteasome pathway controls the level of the transgenic protein. Mol Cell Biol 25: 5270–5281.
31. Wang W, Malcolm BA (1999) Two-stage PCR protocol allowing introduction of multiple mutations, deletions and insertions using QuikChange Site-Directed Mutagenesis. Biotechniques 26: 680–682.
32. Koinuma D, Shinozaki M, Komuro A, Goto K, Saitoh M, et al. (2003) Arkadia amplifies TGF-beta superfamily signalling through degradation of Smad7. Embo J 22: 6458–6470.
33. Daniels MJ, Marson A, Venkitaraman AR (2004) PML bodies control the nuclear dynamics and function of the CHFR mitotic checkpoint protein. Nat Struct Mol Biol 11: 1114–1121.
34. Martinez R, Setien F, Voelter C, Casado S, Quesada MP, et al. (2007) CpG island promoter hypermethylation of the pro-apoptotic gene caspase-8 is a common hallmark of relapsed glioblastoma multiforme. Carcinogenesis.
35. Tokunaga E, Oki E, Nishida K, Koga T, Yoshida R, et al. (2006) Aberrant hypermethylation of the promoter region of the CHFR gene is rare in primary breast cancer. Breast Cancer Res Treat 97: 199–203.
36. Littlepage LE, Ruderman JV (2002) Identification of a new APC/C recognition domain, the A box, which is required for the Cdh1-dependent destruction of the kinase Aurora-A during mitotic exit. Genes Dev 16: 2274–2285.
37. Crane R, Kloepfer A, Ruderman JV (2004) Requirements for the destruction of human Aurora-A. J Cell Sci 117: 5975–5983.
38. Kawai H, Wiederschain D, Yuan ZM (2003) Critical contribution of the MDM2 acidic domain to p53 ubiquitination. Mol Cell Biol 23: 4939–4947.
39. Kawai H, Lopez-Pajares V, Kim MM, Wiederschain D, Yuan ZM (2007) RING domain-mediated interaction is a requirement for MDM2's E3 ligase activity. Cancer Res 67: 6026–6030.
40. Takai R, Matsuda N, Nakano A, Hasegawa K, Akimoto C, et al. (2002) EL5, a rice N-acetylchitooligosaccharide elicitor-responsive RING-H2 finger protein, is a ubiquitin ligase which functions in vitro in co-operation with an elicitor-responsive ubiquitin-conjugating enzyme, OsUBC5b. Plant J 30: 447–455.
41. Matsuda N, Suzuki T, Tanaka K, Nakano A (2001) Rma1, a novel type of RING finger protein conserved from Arabidopsis to human, is a membrane-bound ubiquitin ligase. J Cell Sci 114: 1949–1957.
42. Matsuda N, Kitami T, Suzuki T, Mizuno Y, Hattori N, et al. (2006) Diverse effects of pathogenic mutations of Parkin that catalyze multiple monoubiquitylation in vitro. J Biol Chem 281: 3204–3209.
43. Privette LM, Gonzalez ME, Ding L, Kleer CG, Petty EM (2007) Altered expression of the early mitotic checkpoint protein, CHFR, in breast cancers: implications for tumor suppression. Cancer Res 67: 6064–6074.
44. Morioka Y, Hibi K, Sakai M, Koike M, Fujiwara M, et al. (2006) Aberrant methylation of the CHFR gene is frequently detected in non-invasive colorectal cancer. Anticancer Res 26: 4267–4270.

Carcinogenesis vol.29 no.4 pp.834–839, 2008
doi:10.1093/carcin/bgn051
Advance Access publication February 17, 2008

Protective versus promotional effects of white tea and caffeine on PhIP-induced tumorigenesis and β-catenin expression in the rat

Rong Wang[1], W.Mohaiza Dashwood[1], Christiane V.Löhr[2], Kay A.Fischer[2], Clifford B.Pereira[3], Mandy Louderback[1], Hitoshi Nakagama[4], George S.Bailey[1], David E.Williams[1,5] and Roderick H.Dashwood[1,5,*]

[1]Linus Pauling Institute, [2]College of Veterinary Medicine and [3]Department of Statistics, Oregon State University, Corvallis, OR 97331, USA, [4]Biochemistry Division, National Cancer Center Research Institute, 1-1, Tsukiji 5-chome, Chuo-ku, Tokyo 104-0045, Japan and [5]Department of Environmental and Molecular Toxicology, Oregon State University, Corvallis, OR 97331, USA

*To whom correspondence should be addressed. Tel: +1 541 737 5086; Fax: +1 541 737 5077;
Email: Rod.Dashwood@oregonstate.edu

A 1 year carcinogenicity bioassay was conducted in rats treated with three short cycles of 2-amino-1-methyl-6-phenylimidazo[4,5-*b*]pyridine (PhIP)/high-fat (HF) diet, followed by 2% white tea (wt/vol), 0.05% epigallocatechin-3-gallate (EGCG) or 0.065% caffeine as sole source of fluid intake. Thirty-two percent of the PhIP/HF controls survived to 1 year, compared with 50, 48.7 and 18.2% in groups given white tea, EGCG and caffeine, respectively. After 1 year, PhIP/HF controls had tumors in the colon, skin, small intestine, Zymbal's gland, salivary gland and pancreas. For all sites combined, excluding the colon, tumor incidence data were as follows: PhIP/HF 69.5%, PhIP/HF + EGCG 48.7%, PhIP/HF + white tea 46.9% and PhIP/HF + caffeine 13.3%. Unexpectedly, a higher incidence of colon tumors was detected in rats post-treated with white tea (69%) and caffeine (73%) compared with the 42% incidence in PhIP/HF controls. In the colon tumors, β-catenin mutations were detected at a higher frequency after caffeine posttreatment, and there was a shift toward more tumors harboring substitutions of Gly34 with correspondingly high protein and messenger RNA expression seen for both β-catenin and c-Myc. c-Myc expression exhibited concordance with tumor promotion, and there was a concomitant increase in cell proliferation versus apoptosis in colonic crypts. A prior report described suppression of PhIP-induced colonic aberrant crypts by the same test agents, but did not incorporate a HF diet. These findings are discussed in the context of epidemiological data which do not support an adverse effect of tea and coffee on colon tumor outcome—indeed, some such studies suggest a protective role for caffeinated beverages.

Introduction

It is now well established that human colorectal cancers contain mutations that stabilize the β-catenin protein, causing constitutive activation of β-catenin/T-cell factor (Tcf) signaling and overexpression of downstream targets, such as c-Myc, c-Jun and cyclin D1 (1). Similar findings have been reported in preclinical models of colon cancer. For example, carcinogen-induced rat colon tumors contain oncogenic mutants of β-catenin that are resistant to degradation via the phosphorylation/ubiquitination/proteosome pathway (2), and β-catenin stabilization constitutively activates c-*myc*, c-*jun* and *cyclin D1* expression in the corresponding tumors (3,4). However, the frequency and spectrum of β-catenin mutations depends on the dosing protocol employed. Continuous feeding of the heterocyclic amine 2-amino-1-methyl-6-phenylimidazo[4,5-*b*]pyridine (PhIP) produced colon tumors with high levels of β-catenin expression (5), and the tumors harbored mutations in either β-catenin or adenomatous polyposis coli (6). When dietary PhIP was given via three short cycles followed by a high-fat (HF) diet, β-catenin protein again was expressed at high levels, but only 55% of the colon tumors harbored β-catenin or adenomatous polyposis coli mutations (7). The spectrum and frequency of β-catenin mutations also can be influenced by post-initiation exposure to phytochemicals. For example, a higher proportion of tumors containing direct substitutions in critical Ser/Thr residues of the β-catenin protein was seen following treatment with indole-3-carbinol and chlorophyllin (3,4).

In the present investigation, we sought to test the post-initiation tumor-suppressing effects of white tea and two of its major constituents, namely caffeine and the polyphenolic compound epigallocatechin-3-gallate (EGCG), in rats treated with PhIP/HF diet. White tea is the least processed type of tea; leaves of *Camellia sinensis* contain polyphenols that undergo increasing oxidation in the conversion of white to green to oolong and finally to black tea (8). Prior studies with white tea showed (i) potent antimutagenic effects against PhIP and other heterocyclic amines in the *Salmonella* assay; (ii) inhibition of β-catenin/Tcf activity *in vitro*; (iii) suppression of intestinal polyps in the Apc^{min} mouse and (iv) protection against PhIP-induced colonic aberrant crypt foci (ACF) in the rat (8–12). In the present report, white tea and caffeine given post-initiation unexpectedly promoted rather than suppressed PhIP-induced colon tumors. Caffeine increased β-catenin and c-Myc expression, altered the spectrum and frequency of β-catenin mutations and augmented cell proliferation while inhibiting apoptosis in colonic crypts.

Materials and methods

Test agents

PhIP was purchased from Toronto Research Chemicals (Ontario, Canada) and prepared as an 8 mg/ml solution in test vehicle (0.8% dimethylsulfoxide in milliQ water, adjusted to pH 3.5 with 0.1 N HCl). AIN-93G, AIN-93M and AIN-93G supplemented with 23% (wt/wt) hydrogenated vegetable oil (HF diet) were obtained from Dyets (Bethlehem, PA). Mutan White tea (referred to hereafter as 'white tea') was provided by Stash Tea Co. (Portland, OR). A solution of 2% (wt/vol) white tea was prepared by brewing loose leaf tea (2 g/100 ml) for 3 min in just-boiled 0.5% citric acid buffer (26 mM, pH 2.7). EGCG (TEAVIGO™, DSM Nutritional Products, Basel, Switzerland) and caffeine (Sigma–Aldrich, St Louis, MO) also were dissolved in 0.5% citric acid buffer, which enhances the stability of tea constituents compared with milliQ water alone. Solutions were prepared fresh every 2–3 days, and the stability of tea constituents was verified by high-performance liquid chromatography, as reported (8). 5-Bromo-2′-deoxyuridine (BrdU; Sigma–Aldrich) was prepared as a 20 mM solution in phosphate-buffered saline (PBS).

Animals and treatments

These studies received prior approval from Oregon State University Institutional Animal Care and Use Committee. Male F344 rats, 3–4 weeks of age, were purchased from the National Cancer Institute and housed in a ventilated, temperature-controlled room at 25°C with a 12 h light–dark cycle. After acclimatization to the basal diet (AIN-93G) for 3 days, rats were treated with three cycles of PhIP/HF diet using a protocol modified from Ubagai *et al.* (7). Specifically, PhIP (50 mg/kg) or vehicle alone was given by oral gavage every day for 2 weeks and rats were fed standard AIN-93G (low fat) diet, and this was followed by 4 weeks on AIN-93G HF diet, during which time no PhIP was administered (Figure 1A). After three such cycles of PhIP/HF treatment, rats were switched to standard AIN-93M diet for the remainder of the study. At this time, rats were randomly assigned to the various treatment groups, namely 2% white tea, 0.05% EGCG, 0.065% caffeine or citrate buffer alone (controls), administered as before (12) as sole source of drinking fluid. Test and vehicle groups initially comprised 40 and 10 rats each, respectively, and survival was followed until the study was terminated at 1 year. Rats were euthanized early due to one of the following signs of morbidity: (i) sudden loss of body weight,

Abbreviations: ACF, aberrant crypt foci; BrdU, 5-bromo-2′-deoxyuridine; *Ctnnb1*, β-catenin gene (rat); EGCG, epigallocatechin-3-gallate; HF, high fat; mRNA, messenger RNA; PBS, phosphate-buffered saline; PCR, polymerase chain reaction; PhIP, 2-amino-1-methyl-6-phenylimidazo[4,5-*b*]pyridine; Tcf, T-cell factor.

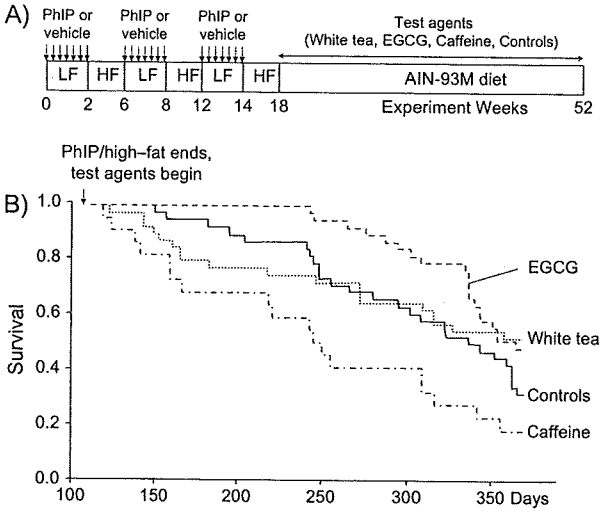

Fig. 1. Dosing protocol and survival curves of rats given PhIP/HF diet followed by white tea, EGCG or caffeine. (**A**) Male F344 rats were fed standard AIN-93G (low fat, LF) diet and given vehicle or PhIP (50 mg/kg) by oral gavage every day for 2 weeks, followed by 4 weeks on AIN-93G supplemented with 23% (wt/wt) hydrogenated vegetable oil (HF diet), during which time no PhIP was administered. After three such cycles, rats were switched to standard AIN-93M diet and given 2% white tea, 0.05% EGCG, 0.065% caffeine or citrate buffer alone (controls) as sole source of drinking fluid. (**B**) Survival curves of animals given PhIP/HF followed by white tea, EGCG or caffeine. The first sign of morbidity was at day 128 in the group post-treated with caffeine (dotted–dashed line). Data shown in the figure are cumulative and include animals that were euthanized before the study was terminated at 1 year.

appetite or fluid intake; (ii) bleeding in the stools over several days and (iii) overt discomfort and breathing difficulty or other signs of malaise. In all cases, rats were euthanized by CO_2 inhalation and a thorough necropsy was performed. One hour before killing, four rats in each group were selected at random to receive an intraperitoneal injection of 200 μmol BrdU/kg body wt.

Histopathology and immunohistochemistry

The following tissues were collected at necropsy: colon, small intestine, pancreas, prostate, lung, liver, kidney, bladder, skin and Zymbal's gland. The colon and small intestine were cleaned with cold PBS and opened longitudinally so as to record the position and size of tumors. Small tumors (<10 mm^3) were fixed whole in 10% formalin, whereas larger tumors were sectioned longitudinally into two or three portions, one of which was fixed in 10% formalin, stained with hematoxylin and eosin and analyzed by light microscopy. Other portions were stored at −80°C for molecular analyses. After tumors were removed, colons from rats treated with BrdU were fixed in 10% buffered formalin and embedded longitudinally in paraffin, from which serial sections were cut for immunostaining.

Immunostaining used the BrdU *in situ* detection kit (BD Bioscience, San Diego, CA) according to the manufacturer's instructions. Sections were dewaxed and rehydrated, and after antigen retrieval with BD™ Retrieval A working solution in a microwave oven (80°C, 10 min) and slow cooling >20 min, slides were blocked for 10 min with 3% H_2O_2, rinsed three times in PBS and incubated with biotinylated anti-BrdU monoclonal antibody (1:40 dilution) for 1 h in a humidified chamber. After reaction with streptavidin peroxidase, sections were stained with Nova Red (Vector Laboratories, Burlingame, CA) and counterstained with hematoxylin.

Cleaved caspase-3 was determined using the EnVision+System–HRP Kit (Dako, Carpinteria, CA). Sections were dewaxed, rehydrated, rinsed with Dako AR buffer and then heated in a pressure cooker (121°C) for 5 min, followed by 20 min cooling at room temperature. After washing with water, endogenous peroxidases were blocked by incubating sections in 3% H_2O_2 in Dako TBST for 10 min, followed by Tris-buffered saline Tween-20 solution (TBST) alone. Sections were blocked with Dako serum-free protein for 10 min and then covered with polyclonal rabbit anticleaved caspase-3 (1:50 dilution in PBS), which specifically detects the endogenous large fragment of cleaved caspase-3 resulting from cleavage adjacent to Asp175 (Cell Signaling Technology, Danvers, MA). Sections were developed with Nova Red for 7 min, rinsed in water and counterstained with hematoxylin.

Labeling indices were determined based on the number of positive cells/total cells per crypt, using at least 45 well-distinguished crypts per rat; that is at least 15 crypts in the distal, middle and proximal regions of the colon. Only complete, well-oriented, longitudinally sectioned crypts with lumen at the top and muscularis mucosae at the base were evaluated.

Immunoblotting

Western analyses of β-catenin and c-Myc, normalized to β-actin, were examined as described before (3,4). In brief, frozen samples of tumors and adjacent normal-looking tissue were thawed and homogenized in lysis buffer, then centrifuged at 15 000 r.p.m. for 5 min and the supernatant (20 μg protein) was separated by sodium dodecyl sulfate–polyacrylamide gel electrophoresis on a 4–12% bis–Tris gel (Novex, Invitrogen, Carlsbad, CA), followed by transfer to nitrocellulose membrane (Invitrogen). Equal protein loading was confirmed by Amido Black staining. The membrane was blocked for 1 h with 2% bovine serum albumin, followed by incubation with primary antibody overnight at 4°C, ending with secondary antibody conjugated with horseradish peroxidase (Bio-Rad, Hercules, CA). Primary antibodies were as reported (3).

Quantitative real-time polymerase chain reaction

Isolation of messenger RNA (mRNA) from tissues and quantification of β-catenin gene (*Ctnnb1*) (rat), *cyclin D1*, *c-myc*, *c-jun* and *glyceraldehyde-3-phosphate dehydrogenase*were performed using the methodology reported by Wang *et al.* (13).

Single-strand conformation polymorphism and direct sequencing

Screening for β-catenin mutations by polymerase chain reaction (PCR)-based single-strand conformation polymorphism analysis coupled with direct sequencing was performed using the methodology reported elsewhere (3,4,13).

Statistics

Tumor incidence and multiplicity (number of tumors/tumor-bearing animal) were compared by logistic regression and non-parametric rank tests, respectively. Student's *t*-test and analysis of variance were used, respectively, for pairwise and group comparisons of molecular data.

Results

Survival was enhanced by EGCG but reduced by caffeine

The concentrations of EGCG and caffeine used here were similar to those present in brewed white tea beverage and did not adversely affect body weights for the first few weeks after the start of their administration; indeed, a slight gain in body weights was detected for the three treatment groups versus the control group, but this was not statistically significant (data not presented). Some of the animals were euthanized early due to the presence of large Zymbal's gland or skin tumors, whereas others suddenly lost appetite and/or body weight and at necropsy presented with colon or other tumors. In the PhIP/HF control group, the first sign of morbidity appeared at day 154, and less than one-third of the animals (32%) survived to the end of 1 year (Figure 1). In the group post-treated with EGCG, the first sign of morbidity was delayed significantly, until day 243, and the overall survival rate at 1 year was 49% ($P = 0.033$ versus PhIP/HF controls, Wilcoxon test). In the group post-treated with caffeine, initial signs of morbidity were seen as early as day 128, and only 18% survived to 1 year ($P = 0.013$ versus PhIP/HF controls). In rats post-treated with white tea, the first sign of morbidity was on day 132, fully 3 weeks before PhIP/HF controls showed morbidity, but 52% survived to 1 year; there was no significant difference overall compared with PhIP/HF controls ($P = 0.580$, trend analysis).

Unexpected promotion of colon tumors by white tea and caffeine

No tumors were detected in any of the vehicle/HF groups when the study was terminated after 1 year, but a broad spectrum of tumors was seen in animals given PhIP/HF diet (Table I). As expected, the colon was the most common target organ, and 41.6% of the PhIP/HF controls developed adenocarcinomas of the colon (Table I). In the same group, the incidence of tumors at other sites after 1 year was as follows: skin 27.8%, small intestine adenocarcinomas 19.4%, Zymbal's gland sebaceous squamous cell carcinomas 11.1%, acinary pancreatic adenocarcinomas 5.6% and salivary gland adenocarcinomas 5.6%. A similar range of tumors was reported before in rats given PhIP, including

Table I. Cumulative incidence of colon and non-colon tumors induced in the rat by three short cycles of PhIP/HF diet, and the effects of EGCG, white tea and caffeine given post-initiation

Tumor site/target organ	PhIP/HF controls (%)	PhIP/HF + EGCG (%)	PhIP/HF + white tea (%)	PhIP/HF + caffeine (%)
Colon (primary target organ)	41.6	43.6	68.5*	73.3*
Non-colon (other tumor sites)				
Skin	27.8	23.1	21.9	6.7
Small intestine	19.4	7.7	12.5	6.7
Zymbal's gland	11.1	7.7	3.1	0
Pancreas	5.6	0	3.1	0
Salivary gland	5.6	0	3.1	0
Bladder	0	2.6	3.1	0
Mammary gland	0	0	3.1	0
All non-colon combined[a]	69.5	48.7	46.9	13.3***

The data shown in the table are cumulative and include animals that were euthanized early before the study was finally terminated at 1 year.
[a]Includes other occasional rare tumors—sarcoma, lymphoma, osteosarcoma and fibrous histocytoma.
*$P < 0.05$, ***$P < 0.001$ versus PhIP/HF controls.

pancreatic tumors (14), although to our knowledge this is the first observation of PhIP-induced salivary gland tumors. Histopathology studies identified a wide spectrum of lesions in the skin, including sebaceous adenoma, sebaceous epithelioma, squamous cell carcinoma, papilloma, keratoacanthoma, cystic basal cell tumor and basal cell carcinoma. PhIP was reported as a prostate carcinogen when fed continuously in the diet for 1 year (15), but no prostate lesions were detected in the present investigation or in a prior study that cycled PhIP/HF (7).

In contrast to our previous findings on PhIP-induced ACF (12), no protective effects were seen for EGCG against the development of colon tumors at 1 year (43.6% final incidence, Table I). Moreover, in rats post-treated with white tea and caffeine, the colon tumor incidence was increased significantly to 68.5 and 73.3%, respectively, compared with 41.6% in the PhIP/HF controls ($P = 0.025$ and 0.039, using the Pearson's chi-square test). Interestingly, however, caffeine posttreatment reduced the tumor incidence in several other target organs; for all non-colon tumors combined, the final cumulative incidence was 13.3% (Table I) compared with 69.5% in the PhIP/HF controls ($P = 0.0003$). The corresponding incidence data for EGCG (48.7%) and white tea (46.9%) were not statistically different from the controls for all non-colon tumors combined.

In addition to the increase in colon tumor incidence, white tea and caffeine (but not EGCG) also increased the colon tumor volume ($P = 0.012$ and 0.009, respectively, versus controls, Figure 2). No significant differences were seen for tumor multiplicity, but the trends were similar; the corresponding data were as follows (colon tumors/colon tumor-bearing animal, mean ± standard error): PhIP/HF controls 1.47 ± 0.19, PhIP/HF + EGCG 1.27 ± 0.14, PhIP/HF + white tea 1.91 ± 1.15 and PhIP/HF + caffeine 2.18 ± 0.50 ($P > 0.05$, for all group comparisons, Wilcoxon test).

Altered frequency and spectrum of β-catenin mutations

We next examined β-catenin mutations in colon tumors using PCR-based single-strand conformation polymorphism analysis followed by direct sequencing. The frequency of β-catenin mutations was similar for controls and groups given EGCG or white tea, but significantly higher in rats post-treated with caffeine (Figure 3A). Specifically, in PhIP/HF controls, 36% (5/14) of the colon tumors harbored β-catenin mutations compared with 79% (11/14) after caffeine posttreatment ($P = 0.022$, Pearson's chi-square test). Although slightly elevated at 47.1% (8/17) and 40% (10/25) in the colon tumors from the rats post-treated with EGCG and white tea, respectively, these mutation frequencies were not significantly different from controls.

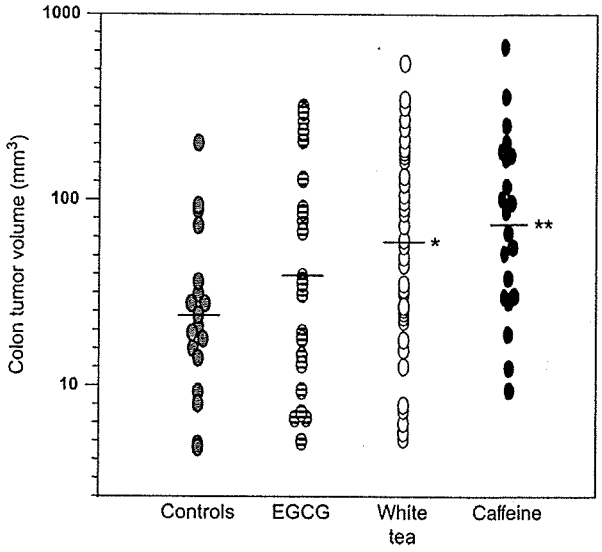

Fig. 2. White tea and caffeine increase colon tumor volume in the rat. Each data point represents a single colon tumor induced by PhIP/HF treatment (see Figure 1A for the dosing protocol). *$P < 0.05$ and **$P < 0.01$ compared with controls. Note that the data include colon tumors from animals that were euthanized early before the study was terminated at 1 year.

In addition to the increase in β-catenin mutation frequency, caffeine also produced a shift in the β-catenin mutation spectrum (Figure 3B). Thus, whereas β-catenin mutations were distributed more or less equally between codons 32 and 34 in controls and in groups given EGCG or white tea, in the colon tumors from rats post-treated with caffeine all but one of the mutations was detected in codon 34, and none were seen in codon 32 (black symbols, Figure 3B). Statistical analyses revealed that caffeine altered the spectrum of β-catenin mutations significantly compared with controls ($P = 0.017$, Fisher's exact test). Codons 32 and 34 represent 'hot spots' in *Ctnnb1* (4) and the corresponding mutations substitute Asp32 and Gly34, which flank Ser33, a key site for phosphorylation/ubiquitination in human and rat β-catenin (1,2).

β-Catenin and its downstream targets—role of c-myc in tumors promoted by tea and caffeine

Immunoblots revealed that β-catenin and c-Myc were more highly expressed in PhIP-induced colon tumors than in adjacent normal-looking tissue (Figure 4A). In addition, mRNA levels of *Ctnnb1*, c-*myc*, c-*jun* and *cyclin D1* were highly overexpressed in colon tumors compared with adjacent normal-looking tissue and in adjacent normal-looking tissue compared with normal colonic mucosa from untreated rats ($P < 0.001$ using Student's *t*-test, see pairwise comparisons indicated in Figure 4B).

The quantitative real-time PCR data were analyzed further, and we observed that colon tumors from rats given white tea or caffeine, but not EGCG, had significantly higher mRNA expression levels of c-*myc* ($P < 0.01$ versus controls, Figure 4C). No such association was seen for *Ctnnb1*, c-*jun* or *cyclin D1* and the posttreatment regimen (data not shown). When plotted as function of the β-catenin mutation status (Figure 4D), mRNA levels of c-*myc* were more highly expressed in colon tumors harboring codon 34 mutations than in tumors with wild-type β-catenin ($P < 0.01$) or codon 32 mutations ($P < 0.05$), and *Ctnnb1* mRNA expression also was higher in tumors with codon 34 mutations than wild-type β-catenin ($P < 0.01$).

Enhanced cell proliferation and reduced apoptosis during colon tumor promotion by white tea and caffeine

Immunostaining for BrdU incorporation revealed an expansion of the colonic crypt zone of cell proliferation in groups post-treated with

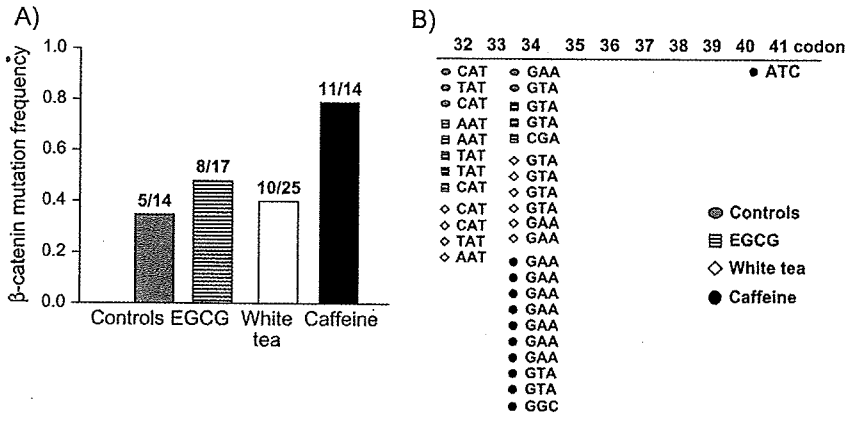

Fig. 3. Altered frequency and spectrum of β-catenin mutations in colon tumors. (**A**) β-Catenin mutations were screened by PCR-based single-strand conformation polymorphism analysis and direct sequencing, as before (3,4,13). Incidence data show the number of confirmed mutations/total samples analyzed by single-strand conformation polymorphism, above each corresponding bar. (**B**) Mutations were localized almost exclusively to codons 32 and 34 of the *Ctnnb1*, except for a codon 41 mutation in the caffeine group, which also completely lacked the codon 32 mutants detected in other groups. Data shown in the figure include colon tumors from animals that were euthanized before the study was terminated at 1 year.

caffeine and white tea, but not EGCG. The BrdU-labeling index, determined for the entire crypt column, was 12.1 ± 1.1% and 13.3 ± 0.5% in rats post-treated with white tea and caffeine, respectively, and augmented significantly versus 9.7 ± 0.9% in the PhIP/HF controls ($P < 0.05$, Figure 5A). The corresponding index for cleaved caspase-3, a measure of apoptosis, was 1.11 ± 0.38% and 0.68 ± 0.19% in rats post-treated with white tea and caffeine, respectively, which was significantly <2.44 ± 0.43% in the controls ($P < 0.05$ and $P < 0.01$, respectively, Figure 5B). Upon closer inspection, apoptotic cells were located mainly in the extreme apical crypt region for controls, but further down the crypt in rats post-treated with caffeine (Figure 5B). Cell proliferation and apoptosis indices were unaffected by posttreatment with EGCG. It is noteworthy that in rats given vehicle (no PhIP) and post-treated with white tea or caffeine, but not EGCG, the apoptosis index also was attenuated significantly versus the corresponding controls (data not presented).

Discussion

Ubagai *et al.* (7) described a protocol for the efficient induction of large intestine tumors in the rat by intermittent administration of PhIP and a HF diet. Specifically, 2 weeks of PhIP treatment at 400 p.p.m. in the diet were followed by 4 weeks of HF diet, which was repeated three times, ending with continuous feeding of HF diet for 42 weeks—this regimen produced a final incidence of large intestine tumors similar to that seen with continuous dietary PhIP treatment for an entire year (7). Although it reduced dramatically the amount of PhIP needed to produce colon tumors in the rat, we modified the protocol in order to further optimize carcinogen use. We also sought to eliminate HF exposure in the latter part of the study to facilitate post-initiation experiments with phytochemicals. Thus, PhIP was given by oral gavage at a dose (50 mg/kg body wt/day) that was matched to the daily carcinogen intake from 400 p.p.m. PhIP in the diet, and after three such cycles of PhIP/HF treatment, standard AIN-93M diet rather than HF diet was given until the study was terminated at 1 year. Using this modified protocol, the colon tumor incidence was 41.6%, comparable with the 45% incidence reported by Ubagai *et al.* (7). Animals in the PhIP/HF control group developed a wide spectrum of tumors (Table I) and less than one-third survived tumor free for 1 year (Figure 1). Rats were euthanized early due to the presence of Zymbal's gland tumors and/or skin lesions or after the appearance of blood in the stools, which was usually indicative of bleeding into the gastrointestinal tract from one or more tumors in the large or small intestine.

We reported previously (12) that white tea, EGCG and caffeine protected in the rat against PhIP-induced ACF, which are putative preneoplastic lesions and used as biomarkers of final colon tumor outcome (16–18). However, in the present investigation, EGCG had no inhibitory effect, and white tea and caffeine promoted rather than suppressed colon tumors. It is unclear whether this reflects a basic limitation of ACF as biomarkers of tumor outcome, as reported by others for genistein and cholic acid (19–21), or alternatively that caffeine and white tea exert a true biphasic response in the rat colon, being beneficial (protective) during short-term treatment but deleterious (promotional) after prolonged exposure. Importantly, however, we observed that caffeine offered significant protection in other target organs of PhIP-induced tumorigenesis (Table I). The cumulative results include animals that died early, but the overall trends were similar in each of the treatment groups for rats that survived to 1 year (data not shown). We interpret this as evidence that protection by caffeine in other target organs was real, and not due to fewer rats surviving to 1 year. Previously (22), caffeine was reported to protect against PhIP-induced mammary tumors in female rats but also promoted tumor formation in the colon.

Consistent with their tumor-promoting activities, caffeine and white tea altered colonic crypt homeostasis by enhancing cell proliferation versus apoptosis (Figure 5). Similar findings were obtained before in rats given chlorophyllin or indole-3-carbinol, and colon tumor promotion was associated with a shift in the β-catenin mutation spectrum (3,4). Thus, we rationalized that a likely mechanism for tumor promotion by white tea and caffeine might be via the dysregulation of β-catenin/Tcf signaling since β-catenin mutation and increased β-catenin expression are clearly associated with tumor progression (1). An increase in β-catenin mutations thus would be consistent with enhanced tumor growth by caffeine and white tea.

An increase in β-catenin mutation frequency coupled with a shift in the β-catenin mutation spectrum indeed was observed in colon tumors from rats post-treated with caffeine, but not white tea, indicating that β-catenin mutation status alone could not explain the promotional activities seen here. The colon tumors from rats given caffeine harbored codon 34 β-catenin mutants at a higher frequency than codon 32 mutants, suggesting that one or more promotional mechanisms 'selected' certain oncogenic forms of β-catenin to progress in preference to others. We do not know the reason for this apparent selection pressure, given that oncogenic β-catenin mutants with substitutions at either Asp32 or Gly34 were equally effective in activating a β-catenin/Tcf-responsive reporter construct (3,23).

Downstream targets of β-catenin/Tcf were highly expressed in colon tumors, namely c-*myc*, c-*jun* and *cyclin D1* and so too was *Ctnnb1* mRNA itself. Overexpression of β-catenin protein therefore might arise due to mutational events that stabilize the β-catenin protein

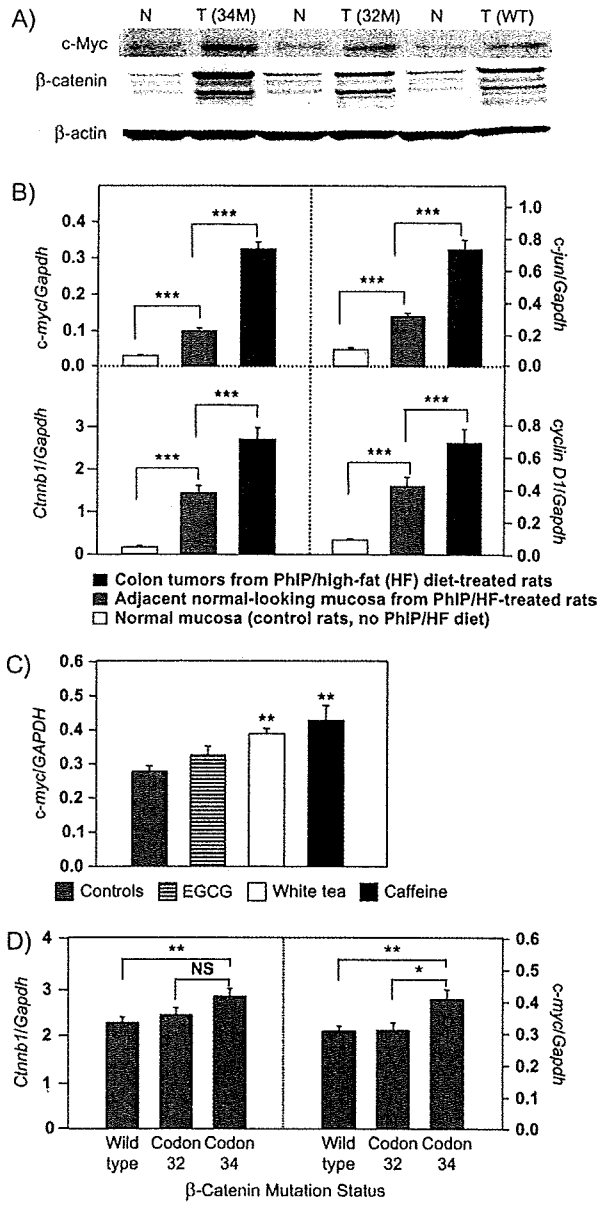

Fig. 4. Overexpression of β-catenin and β-catenin/Tcf target genes in rat colon tumors induced by PhIP/HF treatment. (**A**) Immunodetection of β-catenin and c-Myc in colon tumors (T) and adjacent normal-looking tissue (N). The loading control was β-actin. Blots shown are representative data from more than a dozen tumors, each with mutations in *Ctnnb1* codon 32 (32M), codon 34 (34M) or wild-type (WT), respectively. (**B**) Quantitative real-time PCR was used to examine *Ctnnb1*, c-*myc*, c-*jun* and *cyclin D1* mRNA levels, normalized to *glyceraldehyde-3-phosphate dehydrogenase* (*Gapdh*). Data = mean ± standard error, $^{***}P < 0.001$. (**C**) Quantitative real-time PCR data for c-*myc* (mean ± standard error) plotted as a function of posttreatment regimen; $^{**}P < 0.01$ versus controls. No significant differences were seen for the corresponding data on c-*jun*, *cyclin D1* or *Ctnnb1* (data not shown). (**D**) Quantitative real-time PCR data for *Ctnnb1* and c-*myc* (mean ± standard error) plotted as a function of β-catenin mutation status. $^{*}P < 0.05$, $^{**}P < 0.01$; NS, not significant. No significant changes were seen for corresponding data on c-*jun* and *cyclin D1* (data not shown). Data in the figure are cumulative and include colon tumors from animals that were euthanized before the study was terminated at 1 year.

(1) or via dysregulation of *Ctnnb1* expression at the transcriptional level, as reported for 1,2-dimethylhydrazine-induced colon tumors (13). Importantly, among the three β-catenin/Tcf target genes examined, only c-*myc* showed any concordance with tumor promotion by white tea and caffeine (Figure 4C). Thus, rather than β-catenin, c-Myc overexpression may be important in the promotional mechanism of white tea and caffeine. In its capacity as an ataxia telangiectasia mutated/ATM and Rad3-related kinase inhibitor, caffeine was reported to prevent p53 accumulation upon activation of c-Myc or E2F1 (24). We recently described a pathway in which overexpression of c-Myc elevated E2F1 and enhanced Bcl-2 levels, resulting in suppression of apoptosis (25). Suppression of apoptosis in the present study was evident for caffeine and white tea using cleaved caspase-3 as a biomarker, in animals treated with PhIP/HF diet and also in the negative controls given three cycles of vehicle/HF diet. However, we did not examine the possible role of E2F1, Bcl-2 or p53 in the promotional mechanism of caffeine and white tea in the rat colon, and this is worthy of future study.

Finally, it is important to note that a substantial literature exists on tea and coffee consumption in humans, which does not indicate an adverse effect on tumor outcome—indeed, some studies suggest a protective role for these caffeinated beverages. For example, Tavani *et al.* (26) reviewed epidemiological studies for the period 1990–2003 on coffee, decaffeinated coffee and tea and cancer of the colon and rectum. For coffee consumption, most case–control studies found risk estimates below unity for colon cancer, but no relation for rectal cancer. A meta-analysis of 5 cohort and 12 case–control studies found a pooled relative risk of 0.75 for colon cancer, which was significant. No such relationship was seen for tea or decaffeinated coffee. A more recent meta-analysis (27) concluded that 'despite the strong evidence from *in vitro* and non-human *in vivo* studies in support of green and black tea as potential chemopreventive agents against colorectal cancer, available epidemiologic data are insufficient to conclude that either tea type may protect against colorectal cancer in humans'. In light of the findings from the present investigation and the increased risk for colorectal adenoma associated with meat cooked at high temperature (28), it would be interesting to reassess the epidemiological evidence for possible increased risk of colon cancer in a subset of individuals consuming tea (or coffee) plus large amounts of cooked meat and a HF diet.

In summary, we report here that in rats treated with three short cycles of PhIP/HF diet, post-initiation exposure to white tea and caffeine promoted rather than suppressed colon tumorigenesis, whereas EGCG had no effect. Caffeine increased the frequency of β-catenin mutations, and the colon tumors harbored almost exclusively β-catenin mutants with direct substitutions of Gly34. One important conclusion from these studies is that the final spectrum of β-catenin mutants in colon tumors is clearly influenced by exposure to dietary phytochemicals, as reported before for chlorophyllin and indole-3-carbinol (3,4). There was no direct concordance between the changes in tumor outcome and the expression of β-catenin or its downstream target genes. However, c-Myc was identified as a possible key player in the promotional mechanism of white tea and caffeine. Caffeine protected in other target organs of PhIP-induced tumorigenesis, suggesting a complex pattern of tumor modulation, in line with the general heterogeneity noted in human epidemiology studies of caffeinated beverages.

Supplementary material

The colour version of figure 5 can be found at http://carcin.oxfordjournals.org/

Funding

Inko's White Tea (New York, NY) and National Institutes of Health (CA90890, CA65525 and CA122959); Foundation for Promotion of Cancer Research, Tokyo, Japan to R.H.D.

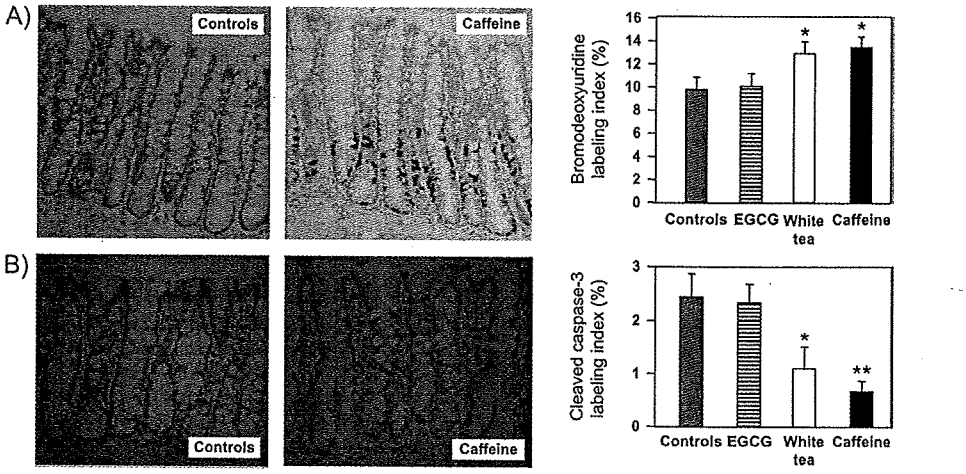

Fig. 5. Cell proliferation and apoptosis in rat colonic mucosa after posttreatment with white tea, EGCG and caffeine. Immunodetection of (**A**) bromodeoxyuridine incorporation and (**B**) cleaved caspase-3, and the corresponding labeling indices determined for the entire colonic crypt. The number of positively stained cells was divided by the total number of cells and multiplied by 100 to obtain 'percent labeling' for the entire crypt. Data = mean ± standard error, $^{*}P < 0.05$. $^{**}P < 0.01$ versus controls (Note: color versions of these images are avaliable as supplementary data on the *Carcinogenesis* website).

Acknowledgements

We thank Barbara Delage, Qingjie Li, Tianwei Yu, Gayle Orner, Valerie Elias, Kate Cleveland and Christine Larsen for assistance with necropsy examinations. Laboratory Animal Service staff are gratefully acknowledged for their help with animal care and maintenance. C.Riegger of DSM Nutritional Products kindly provided the EGCG (TEAVIGO™). Mutan White tea was a generous gift from Stash Tea Co.

Conflict of Interest Statement: None declared.

References

1. Schneikert,J. *et al.* (2007) The canonical Wnt signalling pathway and its APC partner in colon cancer development. *Gut*, **56**, 417–425.
2. Al-Fageeh,M. *et al.* (2004) Phosphorylation and ubiquitination of oncogenic mutants of beta-catenin containing substitutions at Asp32. *Oncogene*, **23**, 4839–4846.
3. Blum,C.A. *et al.* (2001) Beta-Catenin mutation in rat colon tumors initiated by 1,2-dimethylhydrazine and 2-amino-3-methylimidazo[4,5-*f*]quinoline, and the effects of post-initiation treatment with chlorophyllin and indole-3-carbinol. *Carcinogenesis*, **22**, 315–320.
4. Blum,C.A. *et al.* (2003) Mutational analysis of *Ctnnb1* and *Apc* in tumors from rats given 1,2-dimethylhydrazine and 2-amino-3-methylimidazo[4,5-*f*]-quinoline: mutational 'hotspots' and the relative expression of beta-catenin and c-jun. *Mol. Carcinog.*, **36**, 195–203.
5. Sugimura,T. *et al.* (2004) Heterocyclic amines: mutagens/carcinogens produced during cooking of meat and fish. *Cancer Sci.*, **95**, 290–299.
6. Dashwood,R.H. *et al.* (1998) High frequency of beta-catenin (*Ctnnb1*) mutations in the colon tumors induced by two heterocyclic amines in the F344 rat. *Cancer Res.*, **58**, 1127–1129.
7. Ubagai,T. *et al.* (2002) Efficient induction of rat large intestinal tumors with a new spectrum of mutations by intermittent administration of 2-amino-1-methyl-6-phenylimidazo[4,5-*b*]pyridine in combination with a high fat diet. *Carcinogenesis*, **23**, 197–200.
8. Santana-Rios,G. *et al.* (2001) Potent antimutagenic activity of white tea in comparison with green tea in the Salmonella assay. *Mutat. Res.*, **495**, 61–74.
9. Dashwood,W.M. *et al.* (2002) Inhibition of β-catenin/Tcf activity by white tea, green tea, and epigallocatechin-3-gallate (EGCG): minor contribution of H_2O_2 at physiologically relevant EGCG concentrations. *Biochem. Biophys. Res. Commun.*, **296**, 584–588.
10. Orner,G.A. *et al.* (2003) Suppression of tumorigenesis in the Apc^{min} mouse: down-regulation of β-catenin signaling by a combination of tea plus sulindac. *Carcinogenesis*, **24**, 263–267.
11. Santana-Rios,G. *et al.* (2001) Inhibition by white tea of 2-amino-1-methyl-6-phenylimidazo[4,5-*b*]pyridine-induced colonic aberrant crypts in the F344 rat. *Nutr. Cancer*, **41**, 98–103.
12. Carter,O. *et al.* (2007) Comparison of white tea, green tea, epigallocatechin-3-gallate and caffeine as inhibitors of PhIP-induced colonic aberrant crypts in the rat. *Nutr. Cancer*, **58**, 60–65.
13. Wang,R. *et al.* (2006) Tumors from rats given 1,2-dimethylhydrazine plus chlorophyllin or indole-3-carbinol contain transcription changes in β-catenin that are independent of the β-catenin mutation status. *Mutat. Res.*, **601**, 11–18.
14. Ogawa,K. *et al.* (1998) Modification by 2-amino-1-methyl-6-phenylimidazo[4,5-*b*]pyridine (PhIP) of 3,2'-dimethyl-4-aminobiphenyl (DMAB)- induced rat pancreatic and intestinal tumorigenesis. *Cancer Lett.*, **124**, 31–37.
15. Shirai,T. *et al.* (1997) The prostate: a target organ for carcinogenicity of 2-amino-1-methyl-6-phenylimidazo[4,5-*b*]pyridine (PhIP) derived from cooked foods. *Cancer Res.*, **57**, 195–198.
16. Bird,R.P. *et al.* (2000) The significance of aberrant crypt foci for understanding the pathogenesis of colon cancer. *Toxicol. Lett.*, **112–113**, 395–402.
17. Stevens,R.G. *et al.* (2007) Epidemiology of colonic aberrant crypt foci: review and analysis or existing studies. *Cancer Lett.*, **252**, 171–183.
18. Corpet,D.E. *et al.* (2002) Most effective colon cancer chemopreventive agents in rats: a systematic review of aberrant crypt foci and tumor data, ranked by potency. *Nutr. Cancer*, **43**, 1–21.
19. Pereira,M.A. *et al.* (1994) Use of azoxymethane-induced foci of aberrant crypts in rat colon to identify potential cancer chemopreventive agents. *Carcinogenesis*, **15**, 1049–1054.
20. Rao,C.V. *et al.* (1997) Enhancement of experimental colon cancer by genistein. *Cancer Res.*, **57**, 3717–3722.
21. Shirtliff,N. *et al.* (1996) Growth features of aberrant crypt foci that resist modulation by cholic acid. *Carcinogenesis*, **17**, 2093–2096.
22. Hagiwara,A. *et al.* (1999) Organ- dependent modifying effects of caffeine, and two naturally occurring antioxidants alpha-tocopherol and n-tritriacontane-16,18-dione, on 2-amino-1-methyl-6-phenylimidazo[4,5-b]pyridine (PhIP)-induced mammary and colonic carcinogenesis in female F344 rats. *Jpn. J. Cancer Res.*, **90**, 399–405.
23. Porfiri,E. *et al.* (1997) Induction of a beta-catenin-LEF-1 complex by wnt-1 and transforming mutants of beta-catenin. *Oncogene*, **15**, 2833–2839.
24. Lindstrom,M.S. *et al.* (2003) Myc and E2F1 induce p53 through p14ARF-independent mechanisms in human fibroblasts. *Oncogene*, **22**, 4993–5005.
25. Li,Q. *et al.* (2007) Bcl-2 over-expression in PhIP-induced colon tumors: cloning of the rat *Bcl-2* promoter and characterization of a pathway involving β-catenin, c-Myc and E2F1. *Oncogene*, **26**, 6194–6202.
26. Tavani,A. *et al.* (2004) Coffee, decaffeinated coffee, tea and cancer of the colon and rectum: a review of epidemiological studies, 1999–2003. *Cancer Causes Control*, **15**, 743–757.
27. Sun,C.L. *et al.* (2006) Green tea, black tea and colorectal cancer risk: a meta-analysis of epidemiologic studies. *Carcinogenesis*, **27**, 1301–1309.
28. Sinha,R. *et al.* (2005) Meat, meat cooking methods and preservation, and risk of colorectal adenoma. *Cancer Res.*, **65**, 8034–8041.

Received January 16, 2008; revised February 4, 2008; accepted February 8, 2008

J Pharmacol Sci 105, 129 – 132 (2007)

Journal of Pharmacological Sciences

Forum Minireview

Life Style-Related Diseases of the Digestive System: Colorectal Cancer as a Life Style-Related Disease: from Carcinogenesis to Medical Treatment

Hirokazu Takahashi[1], Kyoko Yoneda[1], Ayako Tomimoto[1], Hiroki Endo[1], Toshio Fujisawa[1], Hiroshi Iida[1], Hironori Mawatari[1], Yuichi Nozaki[1], Tamon Ikeda[1], Tomoyuki Akiyama[1], Masato Yoneda[1], Masahiko Inamori[1], Yasunobu Abe[1], Satoru Saito[1], Atsushi Nakajima[1,*], and Hitoshi Nakagama[2]

[1]*Gastroenterology Division, Yokohama City University Graduate School of Medicine, 3-9 Fuku-ura, Kanazawa-ku, Yokohama 236-0004, Japan*
[2]*Biochemistry Division, National Cancer Center Research Institute, Tokyo 104-0045, Japan*

Received July 10, 2007; Accepted September 10, 2007

Abstract. Life style-related diseases are associated with an increased risk of colorectal cancer (CRC). Recently, an association has been demonstrated between obesity and CRC. CRC has been associated with markers of insulin or glucose control, and insulin resistance might be the unifying mechanism by which several risk factors affect colorectal carcinogenesis. We evaluated the association between the number of aberrant crypt foci (ACF) and obesity, insulin resistance, hyperlipidemia, and other factors of life style-related disease. As a result, age, body mass index (BMI), waist circumference, and visceral fat obesity were significantly associated with the number of ACF. These results suggest that visceral fat obesity is an important target for CRC prevention. Peroxisome proliferator-activated receptor gamma (PPARγ) is a member of the nuclear receptor superfamily and is highly expressed in CRC. PPARγ ligand administration for 1 to 8 months significantly reduced the number of ACF in human subjects. PPARγ ligand is a promising candidate as a chemopreventive agent. Further investigation is needed to elucidate these mechanisms.

Keywords: life style-related disease, colorectal cancer, chemoprevention, aberrant crypt foci (ACF), peroxisome proliferator-activated receptor gamma (PPARγ)

Introduction

A diet rich in fat and calories and low intake of vegetable, fruits, and fibers are referred to as a Western diet. Chronic conditions including obesity, diabetes, hyperlipedemia, hypertension, and cardiovascular disease have been shown to be associated with a Western diet, alcohol intake, and smoking. Indeed, obesity has been reported to be associated with an elevated risk of cardiovascular disease, diabetes, and mortality (1 – 4). Especially, visceral fat obesity is increasing and is becoming a significant social problem. Recently, these life styles have also been shown to be correlated with increase in colorectal cancer (CRC) risk.

CRC is a disease with a high mortality and morbidity rate, and currently, its prevalence has been increasing worldwide. On the other hand, CRC is potentially one of the most preventable malignancies (5, 6). Correction of the life styles mentioned above may have a major potential for CRC prevention. On the other hand, early detection of CRC or CRC precursor lesions may be promoted by screening of the population at high risk. In addition, chemoprevention, the use of medications to prevent disease, has now been extensively explored in CRC. Some of these interventions, such as supplemental fibers, calcium supplementation, aspirin, nonsteroidal anti-inflammatory drugs (NSAIDs), and selective cyclooxygenase (COX)-2 inhibitors, have been shown to have a potential to reduce both CRC and colorectal adenomas. CRC is thought to progress through several morpho-

*Corresponding author. nakajima-tky@umin.ac.jp
Published online in J-STAGE: October 6, 2007
doi: 10.1254/jphs.FM0070022

logical stages, from the formation of adenomatous polyps to malignant conversion (7). Genetic alterations including mutations in the *APC, K-ras*, and *p53* genes have been reported to accompany the disease progression (8). The earliest identifiable lesion in this pathway may be the aberrant crypt foci (ACF). ACF are prepolyp abnormalities identified in single crypts by magnifying colonoscopy after the administration of methlyene blue dye. Therefore, ACF may be a surrogate marker of CRC, and analysis of the association between clinicopathological variables and ACF formation may be of great significance.

Diabetes, obesity, and CRC

Diabetes, obesity, hyperinsulinemia, and insulin resistance have been repeatedly shown to be associated with CRC (9 – 14). Diabetes was associated with an increased risk for CRC in cohort studies, in accordance with previous studies that demonstrated that diabetes is a moderate risk factor for CRC. Overweight, obesity, or high BMI has been consistently associated with increased risk for CRC incidence and mortality, at least in men and premenopausal women (15 – 18). The WHO definition of the life style-related disease allows the use of a body mass index (BMI) of at least 30 kg/m^2 instead of waist circumference or waist-to-hip ratio (19).

ACF as a biomarker of CRC

ACF, which represent clusters of aberrant colorectal crypts, were first discovered in mice treated with azoxymethane (20). ACF have been demonstrated to be precursor lesions of CRC, and with further investigations, ACF have been established as a biomarker of the risk of CRC in azoxymethane-treated mice and rats (21). In humans, the relationship between ACF and CRC is less clear. The number of ACF was measured using magnifying endoscopy, but the association between ACF and CRC was only partially evident. ACF, however, are also thought to be precursor lesions of colorectal adenoma and CRC in humans (22). Many factors are known to be associated with increased or decreased risk of CRC. Among them, only history of adenomas, age, and the use of NSAIDs have been examined in relation to the development of ACF. The relationships of other factors to the occurrence of ACF in the colon remain unknown.

In the rat model, the formation of ACF was enhanced by cancer promoters and suppressed by chemopreventive agents (23). ACF has also been reported in colonic mucosa in humans (24, 25). Patients with CRC had more ACF with *K-ras* mutations than those without CRC. These results suggest that ACF are not only morphologically but also genetically distinct lesions and are precursors of adenoma and CRC.

Table 1. Relationships between selected risk factors for colorectal cancer and the number of ACF in the colorectum

Risk factors	Correlation coefficient	*P*-value
Age (years)	0.256	0.0121*
BMI	0.263	0.0044*
Waist (cm)	0.370	0.0003*
Fasting blood sugar	0.021	0.7575
HOMA-IR	0.263	0.6174
Total cholesterol	0.263	0.4771
Triglyceride	0.263	0.2049
VFA (cm^2)	0.512	<0.0001*
SFA (cm^2)	0.108	0.2091

*P-values <0.05 were considered to denote statistical significance. HOMA-IR: homeostasis model assessment of insulin resistance.

ACF and visceral fat obesity

The association between the number of ACF and age, BMI, waist circumference, diabetes, serum lipid, visceral fat area (VFA), and subcutaneous fat area (SFA) were evaluated (Table 1). Our findings indicate that age, BMI, waist circumference, and VFA were significantly associated with the number of ACF. Especially, VFA was strongly associated with the number of ACF. Visceral fat tissue is known as an endocrine organ that secretes adipocytokines such as TNF-α, leptin, and adiponectin. These adipocytokines and/or the visceral fat itself may play an important role in colon carcinogenesis. The number of ACF increased with age. Genetic and epigenetic alterations accumulate with advancing of age; therefore, the increased risk of ACF formation with age may be mainly influenced by these genetic alterations.

Chemoprevention for CRC

Chemoprevention, the use of medications to prevent disease, has now been extensively explored in CRC. Supplemental fibers, calcium supplementation, aspirin, NSAIDs, and selective COX-2 inhibitors have a potential to reduce both CRC and colorectal adenomas. Higher doses and longer durations of use of NSAIDs and COX-2 inhibitors seem to be associated with greater protection from CRC and adenoma. However, these agents are associated with significant cardiovascular events and/or gastrointestinal damage. The balance of benefits to risk does not favor chemoprevention by these